Available online at www.sciencedirect.com
SCIENCE DIRECT®
Precambrian Research 133 (2004) 143–173
Precambrian Research
www.elsevier.com/locate/precamres

Geochronology of a Late Archaean flood basalt province in the Pilbara Craton, Australia: constraints on basin evolution, volcanic and sedimentary accumulation, and continental drift rates☆

T.S. Blake [a,*], R. Buick [b], S.J.A. Brown [c], M.E. Barley [d]

[a] *86 Reservoir Street, Chidlow, WA 6556, Australia*
[b] *Department of Earth and Space Sciences and Astrobiology Program, University of Washington, Seattle, WA 98195-1310, USA*
[c] *Douglas Partners Pty Ltd, 96 Hermitage Road, West Ryde, NSW 2114, Australia*
[d] *School of Earth and Geographical Sciences, The University of Western Australia, 35 Stirling Highway, Crawley, WA 6009, Australia*

Received 23 July 2003; accepted 30 March 2004

Abstract

Eleven high precision (±2–5 million years) SHRIMP zircon U–Pb ages have been obtained from felsic rocks within a single stratigraphic section of late Archaean volcanic and sedimentary rocks in the east Pilbara of Western Australia. The stratigraphic succession (Nullagine and Mount Jope Supersequences in sequence-stratigraphic terminology, Fortescue Group in lithostratigraphic terminology) is interpreted to be the rock record of three major geotectonic cycles that formed in an extensional, rift-related environment between about 2772 and 2715 Ma. The geochronology is constrained by a detailed stratigraphic framework based on unconformities and supported by a preliminary magnetostratigraphy. Field mapping, geochemical and petrographic studies have shown that previously unrecognised thin felsic tuff bands are interbedded in subaerial flood basalt piles and mafic tuffs. While flood basalts and proximal felsic volcanic rocks comprise by volume most of the volcanogenic components of the succession, felsic volcanism is now known to have been active periodically through each geotectonic cycle. The succession covers a time period of about 57 million years. The lower ∼1400 m of a thick (∼1700 m) clastic sedimentary succession from the oldest geotectonic cycle was deposited at a rate of about 100 m per million years over a mean time period of 14 million years. In contrast, a younger ∼150 m thick cogenetic tuff-basalt unit accumulated in less than 3 million years, and others probably accumulated at similar rates, comparable to those of Phanerozoic flood basalts. Unconformities in the succession are shown to be of variable duration and one unconformity marking the boundary between the first and second geotectonic cycles may represent a time-gap of more than 10 million years. The unconformity-based stratigraphic framework, the new geochronology and palaeomagnetic studies [J. Geophys. Res. 108 (2003) B12, 2551, EMP 2-1 to 2-21] have been combined to determine a possible late Archaean continental drift rate for one part of the succession, implying a period of motion as fast as or up to five times faster than any known from the Phanerozoic.

Keywords: Archaean; Geochronology; Flood basalts; Felsic volcanism; Stratigraphy; Basin evolution; Continental drift; Pilbara; Australia

1. Introduction

Reliable geochronology has, over the past two decades, revolutionised the study of Archaean geology. It has allowed the accurate determination of time relationships between rock units that were

☆ Supplementary data associated with this article (Appendices I–III) can be found, in the online version, at doi:10.1016/j.precamres.2004.03.012.

* Corresponding author. Fax: +61-8-9572-3392.
E-mail address: timblake@iinet.net.au (T.S. Blake).

0301-9268/$ – see front matter © 2004 Elsevier B.V. All rights reserved.
doi:10.1016/j.precamres.2004.03.012

previously poorly constrained because of the absence of a biostratigraphy. Thus, it can potentially also provide insights into the early rates of some geological processes and secular changes in those rates over the course of Earth's history.

In suitable Archaean volcanic successions, where there is a high frequency of felsic rocks containing zircons amenable to precise U–Pb isotopic dating, the power of high-resolution geochronology can potentially be coupled with well-resolved stratigraphy to address issues of global geological importance. To date, most such detailed geochronology has been performed in the Superior Craton of Canada. It has been used, amongst other things, to determine the duration of volcanic construction (e.g., Mueller and Mortensen, 2002), the speed and style of basin evolution (e.g., Ayer et al., 2002) and the similarity of tectonic processes and environments to modern plate-tectonic analogues (e.g., Skulski and Percival, 1996; Wyman and Hollings, 1998; Scott et al., 2002; Tomlinson et al., 2002). In the Pilbara Craton of northwestern Australia, a single study of a stratified felsic volcanic pile has attempted to reconstruct the temporal evolution of a metallogenic hydrothermal system (Buick et al., 2002).

There are, however, other possible uses and suitable successions for high-resolution geochronology in Archaean volcanic terrains. Some mafic-dominated successions contain felsic rocks that, with care, can be placed in a stratigraphic context. Such circumstances potentially allow study of interactions between mantle and crustal processes in a world with a higher radiogenic heat flux. It is conceivable that, on an Earth with a greater inventory of undecayed radioactive elements and isotopes, basins evolved more rapidly, orogenies were faster and more intense, and plate motions (if plates in the modern sense existed) were speeded up or occurred on a much smaller scale. Perhaps flood basalt provinces were generated after relatively low degrees of lithospheric stretching and crustal thinning, a result of higher temperatures in the upper mantle and more active tectonics, rather than from mantle plumes. All of these issues can, to some extent, be clarified by stratigraphically controlled high-resolution geochronology, as they all require determination of the rates of Archaean geological processes and comparison with modern equivalents.

In this paper, we provide a high-resolution stratigraphic chronology for a late Archaean mafic-dominated volcanic succession in the Pilbara Craton of northwestern Australia. We use this to make a preliminary attempt to answer the following questions. Firstly, were sedimentation rates in late Archaean fault-bounded epicontinental basins, and hence the constraints on extensional basin development, similar to those for basins formed on modern continental crust? Secondly, were time-gaps across non-marine unconformities, and hence depositional continuity in late Archaean continental settings, equivalent to those prevailing today? Third, were the duration and magnitude of late Archaean flood basalt eruptive episodes, and hence the delivery of mantle melts to the Earth's surface, at all like those in younger flood basalt provinces? And fourth, using some preliminary palaeomagnetic data (Strik et al., 2003), were continental drift rates in the late Archaean similar to present? Though the answers to all of these are still somewhat uncertain, the results illustrate the potential productivity of further coupled stratigraphical–geochronological studies in Archaean mafic-volcanic successions for resolving fundamental questions about Earth's early evolution.

2. Study area

The lower succession of the Hamersley Province (LSHP) in northwestern Australia, constituting most of the Fortescue Group as defined lithostratigraphically (e.g., Thorne and Trendall, 2001) or the Nullagine and Mount Jope Supersequences in an unconformity-based stratigraphic framework (Blake and Barley, 1992; Blake, 1993; Table 1 and Fig. 1), is amongst the oldest (ca. 2772–2715 Ma) continental flood basalt provinces on Earth. While its great age has been known for 20 years (Pidgeon, 1984), our understanding of its evolution is still crude. The succession comprises well-exposed mafic and felsic volcanic rocks, subordinate volcanogenic sedimentary rocks and locally thick units of terrigenous sedimentary rocks that are mostly little deformed and of very low metamorphic grade. Because of its spectacular preservation and exposure, it provides a remarkable window into late Archaean mantle and crustal (e.g., Blake, 1984a), sedimentological (e.g., Blake, 1993), volcanological (e.g., Blake, 2001), biological (e.g., Buick, 1992) and atmospheric (e.g., Rasmussen and Buick, 1999) processes.

Table 1
Regional sequence stratigraphic and lithostratigraphic divisions of the late Archaean to early Proterozoic (ca. 2775–2400 Ma) succession in the Pilbara region

UNCONFORMITY BASED FRAMEWORK							LITHOSTRATIGRAPHIC FRAMEWORK			
Mount Bruce Megasequence Set							Mount Bruce Supergroup			
Mega-sequences (Krapez, 1997)	**Super-sequences (Krapez, 1997)**	**Mega-sequences (Blake & Barley, 1992)**	**Super-sequences (Blake & Barley, 1992)**	**Sequences (Goddard, 1992; Blake, 1993; Krapez, 1996)**	**Super-sequences & Packages in Nullagine Synclinorium (Blake, 2001)**		**Members**	**Formations**	**Groups**	**Tectono-Stratigraphic Sequences (Throne and Trendall, 2001)**
1st Order	2nd Order	1st Order	2nd Order	3rd Order	2^{nd} Order	2^{nd}, 3^{rd} or Higher Order				
Hamersley Range Megasequence	Turee Creek Supersequence	**Hamersley Range Megasequence**	Turee Creek Supersequence	Defined				Kazput Fm	**Turee Creek Group**	
								Koolbye Fm		
							Meteorite Bore Mb (part of formation)	Kungarra Formation		
	Brockman Supersequence		Woongarra Supersequence	None yet defined				Boolgeeda Iron Fm	**Hamersley Group**	
								Woongarra Volcanics		
								Weeli Wolli Fm		
			Brockman Supersequence Package	None yet defined			Yandicoogina Shale Mb	Brockman Iron Fm		
							Joffre Mb			
							Whaleback Shale Mb			
							Dales Gorge Mb			
								Mt McRae Shale		
		Exact	Position	Uncertain				Mt Sylvia Fm		
	Carawine Supersequence	**Chichester Range Megasequence**	Marra Mamba Supersequence Package	None yet defined			Bee Gorge Mb	Wittenoom Fm		
							Paraburdoo Mb			
Chichester Range Megasequence	Marra Mamba Supersequence					?	Mount Newman Mb	Marra Mamba Iron Fm		
							Mount MacLeod Mb			
						12	Nammuldi Mb			
							Roy Hill Shale Mb	Jeerinah Fm	**Fortescue Group**	Sequence 4
							Warrie Mb			
					MJ (2)S	8-11	Woodiana Sandstone Mb			
	Mount Jope Supersequence		**Mount Jope Supersequence**	Maddina Seq Package				Maddina Fm		Sequence 3
				Tumbiana Seq	MJ (1)S	7		Tumbiana Fm		
				Kylena Seq				Kylena Fm		
	Nullagine Supersequence		**Nullagine Supersequence**	Hardey Seq Package	NS	1-6		Hardey Fm		Sequence 2
				Mount Roe Seq				Mount Roe Basalt		Sequence 1

Stratigraphic interval covered by the geochronology in this paper is highlighted in grey. Fortescue Group nomenclature is for the northern Pilbara Craton; members are after MacLeod and de la Hunty (1965) and formations are after Thorne and Hickman (1998). Sequence stratigraphic and lithostratigraphic correlations are simplified. MJ(1)S, Mount Jope (1) Supersequence; MJ(2)S, Mount Jope (2) Supersequence; NS, Nullagine Supersequence.

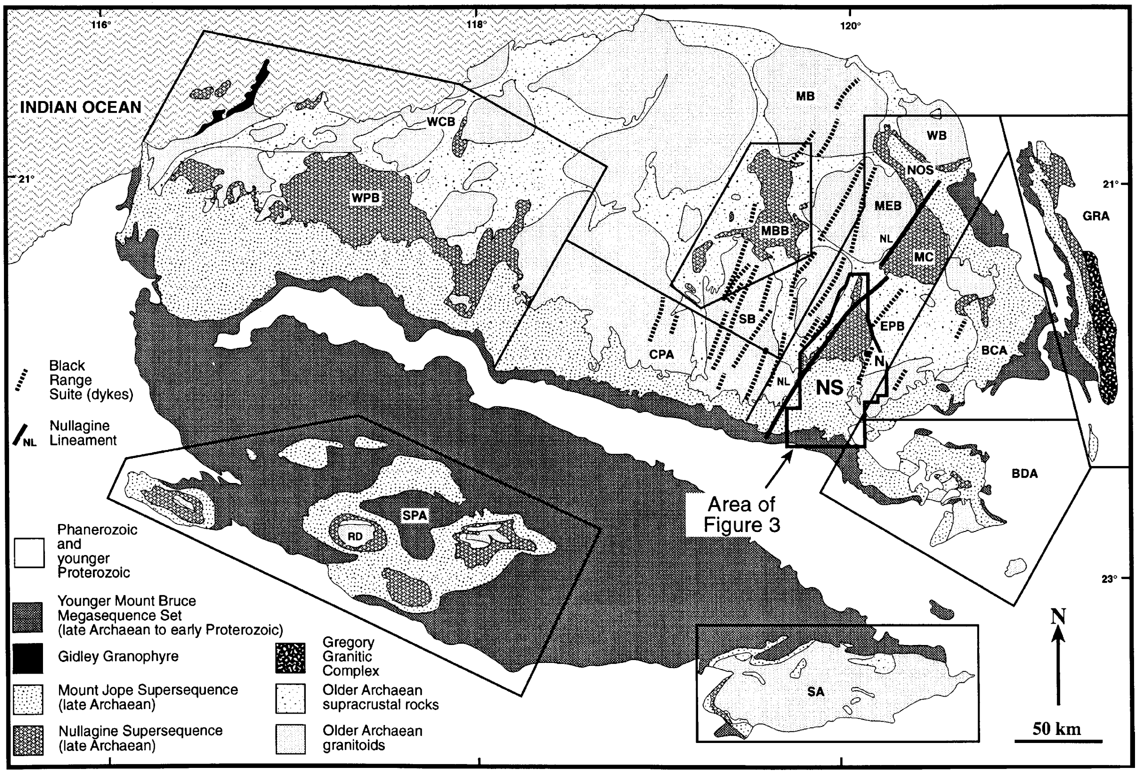

Fig. 1. Simplified geological map of the Pilbara region showing the distribution of components of the Mount Bruce Megasequence Set. The outcrop of the Nullagine and Mount Jope Supersequences is divided into nine areas (after Blake, 1993; BCA, Boodalyerri Creek Area; BDA, Balfour Downs Area; CPA, Central Pilbara Area; EPB, East Pilbara Basin; GRA, Gregory Range Area; MBB, Marble Bar Basin; SA, Sylvania Area; SPA, Southwest Pilbara Area; WPB, West Pilbara Basin). The East Pilbara Basin is divided into three structurally-defined sub-areas (MC, Meentheena Centrocline; NOS, Northwest Oakover Syncline; NS, Nullagine Synclinorium). Other abbreviations: MEB, Mount Edgar Batholith; MB, Muccan Batholith; N, Nullagine; NL, Nullagine Lineament; RD, Rocklea Dome; SB, Shaw Batholith; WB, Warrawagine Batholith; WCB, Whim Creek Belt.

The stratigraphic section of the LSHP studied here is in the Nullagine Synclinorium (Fig. 1). This is a structural remnant of the East Pilbara Basin which is one of at least three late Archaean fault-controlled basins on the northern Pilbara Craton (Blake 1984a,b, 1990a, 1993). Following a mineral exploration program in the 1990's during which the area was re-mapped, it became the focus of stratigraphic

Fig. 2. Summary stratigraphic column (representing a cumulative maximum stratigraphic thickness of about 6 km) of the Nullagine and Mount Jope Supersequences, and lower Marra Mamba Supersequence Package in the Nullagine Synclinorium showing the ages reported herein. The figure includes (from left to right) lithostratigraphic subdivisions (after Hickman and Lipple, 1978; Thom et al., 1979; Thorne and Tyler, 1996), magnetostratigraphy (N, normal; R, reversed; after Strik et al., 2003), dominant lithologies, package (P) and boundary (BD) numbers, a summary of mafic and 'felsic' volcanism (CR, reworked crystal-bearing tuff; CV, crystal vitric tuff; V, vitric tuff; VA, vitric tuff with accretionary lapilli; (∗) not recorded in the Nullagine Synclinorium but present in the Meentheena Centrocline), ages reported herein (except age marked (∗) which is after Wingate, 1999 using the correlation of Blake, 1993, 2001), a summary of the relative duration of unconformities (MT, marine transgression; PS, major shift in palaeomagnetic pole position across boundary), third- or higher-order subdivisions (after Blake, 2001), second-order subdivisions (after Blake, 2001). Estimates of the relative durations of unconformities are based on geological interpretation and geochronology. MMIF, Marra Mamba Iron Formation.

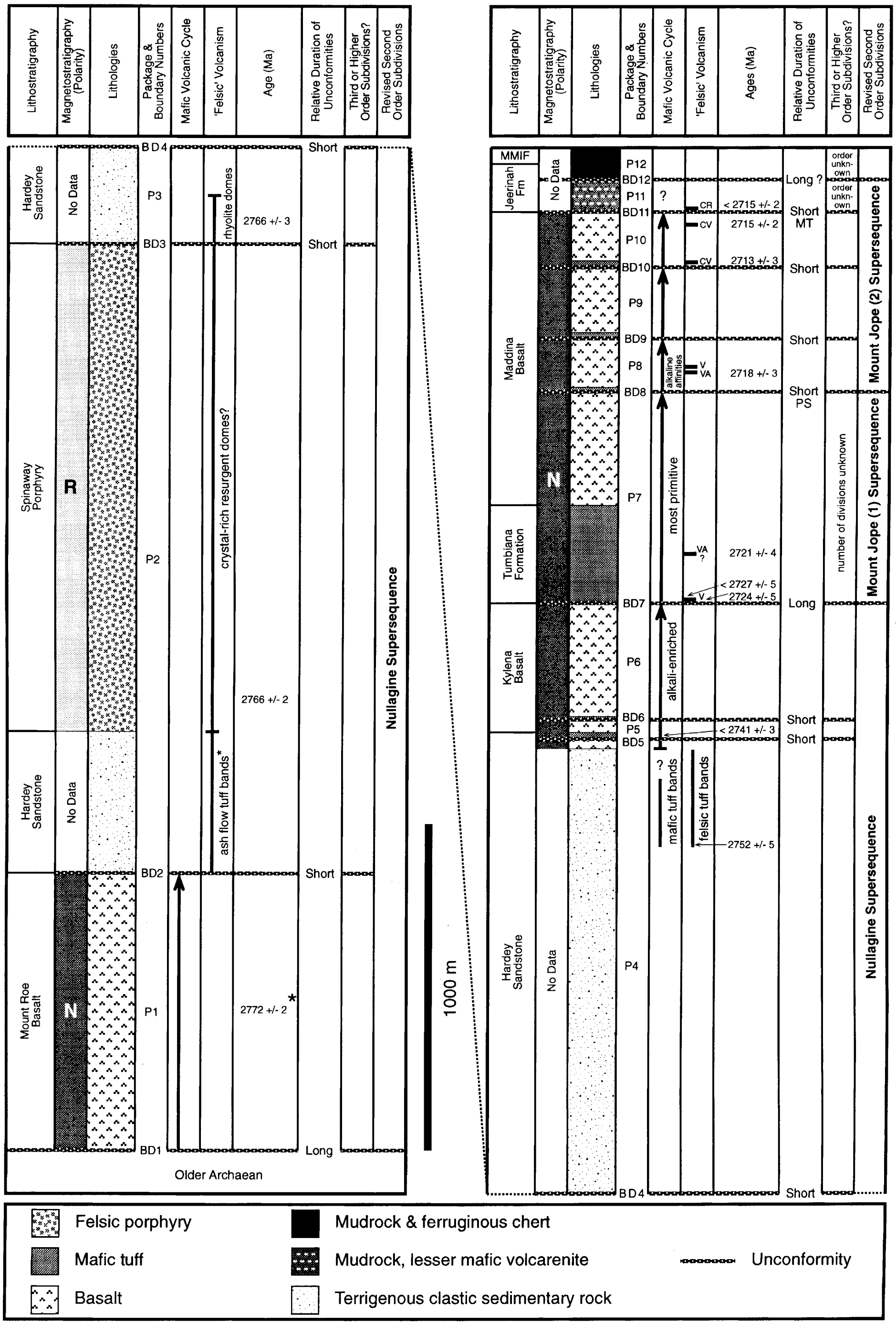
Lithostratigraphy
Magnetostratigraphy (Polarity)
Lithologies
Package & Boundary Numbers
Mafic Volcanic Cycle
'Felsic' Volcanism
Age (Ma)
Relative Duration of Unconformities
Third or Higher Order Subdivisions?
Revised Second Order Subdivisions
Hardey Sandstone
No Data
Spinaway Porphyry
R
Mount Roe Basalt
N
BD4
P3
BD3
P2
BD2
P1
BD1
rhyolite domes
crystal-rich resurgent domes?
ash flow tuff bands*
2766 +/- 3
2766 +/- 2
2772 +/- 2*
Short
Long
Nullagine Supersequence
Older Archaean
1000 m
Ages (Ma)
MMIF
Jeerinah Fm
Maddina Basalt
Tumbiana Formation
Kylena Basalt
P12
BD12
P11
BD11
P10
BD10
P9
BD9
P8
BD8
P7
BD7
P6
BD6
P5
BD5
P4
alkaline affinities
most primitive
alkali-enriched
mafic tuff bands
felsic tuff bands
CR
CV
V
VA
< 2715 +/- 2
2715 +/- 2
2713 +/- 3
2718 +/- 3
2721 +/- 4
< 2727 +/- 5
2724 +/- 5
< 2741 +/- 3
2752 +/- 5
Long ?
Short
MT
PS
order unknown
number of divisions unknown
Mount Jope (2) Supersequence
Mount Jope (1) Supersequence
Felsic porphyry
Mafic tuff
Basalt
Mudrock & ferruginous chert
Mudrock, lesser mafic volcarenite
Terrigenous clastic sedimentary rock
Unconformity

(Fig. 2), sedimentological, volcanological, geochemical and palaeomagnetic studies (Blake, 1990a, 2001; Mann, 1995; Gressier, 1996; Strik, 1998; Strik et al., 2003). Though robust, the stratigraphic framework developed during these studies (Fig. 2) is still relatively unsophisticated in comparison to the level of stratigraphic resolution achieved in many Phanerozoic volcano-sedimentary successions, and future studies will inevitably document more stratigraphic complexity. Nevertheless, the pilot studies of the Nullagine Synclinorium have highlighted far more stratigraphic complexity in the area than was previously supposed (Blake, 1993; Thorne and Hickman, 1998; Thorne and Trendall, 2001; Table 1) and show that a major revision of the regional stratigraphic framework for the entire succession is warranted.

This paper reports the results of a high precision SHRIMP geochronology study of felsic rocks from the Nullagine Synclinorium within the latest stratigraphic framework (Figs. 2 and 3). Importantly, all samples yielding ages are from a single stratigraphic section and there is no ambiguity about their geological context and relative ages. Previous ion microprobe studies of zircons and baddeleyites (Table 2) bracket the terrestrial part of the LSHP between about 2775 and <2715 Ma. However, this temporal framework was compiled using samples from widely spaced geographic locations and its regional stratigraphic significance is entirely dependent on the validity of stratigraphic correlations between disparate sample sites. The prime objective of this study was to avoid this problem by establishing an isotopic age framework for a succession in which there is no ambiguity about the relative ages of geochronology samples. To achieve this, 13 samples were collected from the Nullagine Synclinorium and 1 sample was collected from a mafic dyke that has been correlated geochemically with extrusive rocks in the main sampling area (Fig. 3).

3. Stratigraphic frameworks

A lithostratigraphic framework for rocks in the ca. 2.75–2.40 Ga Hamersley Province (Table 1) was established in the 1960's (e.g., MacLeod et al., 1963; Kriewaldt, 1964; de la Hunty, 1965; MacLeod and de la Hunty, 1966; Kriewaldt and Ryan, 1967; Williams, 1968) with later modifications by Trendall (1979). Since that time the framework has been used, with modifications, on most maps and publications on the geology of the Hamersley Province (e.g., Trendall, 1983, 1990, 1997; Blight, 1985; Arndt et al., 1991; Nelson et al., 1992; Simonson et al., 1993; Thorne and Hickman, 1998). Thorne and Trendall (2001) divided the Fortescue Group into four "Tectono-Stratigraphic Sequences" that mostly follow the divisions of Blake (1993; Table 1). In addition, Thorne and Trendall (2001) re-named the three basins on the northern Pilbara Craton that were first defined and named by Blake (1984a,b; see also 1:100,000 scale maps and legend of Blake, 1990a) and form the basis of Blake (1993, 2001) and Strik (1998) and Strik et al. (2003). The original basin names of Blake (1984a,b) and the definitions and names of other relevant areas of the Pilbara Craton of Blake (1993, fig. 2) are used herein (Fig. 1) because of their historical precedence over the nomenclature of Thorne and Trendall (2001).

An unconformity-based framework for part of the lower succession of LSHP was initiated in the 1980's to early 1990's (Blake, 1984a,b, 1990a,b, 1993), and Blake and Barley (1992) presented a new model for the evolution of the entire Hamersley Province succession based on this work and a reinterpretation of available lithostratigraphic descriptions. The two stratigraphic frameworks and the "Tectono-Stratigraphic Sequences" of Thorne and Trendall (2001) are compared in Table 1.

An unconformity-based framework has not yet been established for all the LSHP, though broad regional divisions were proposed by Blake (1993). However, unconformity-based divisions are most advanced in the Nullagine Synclinorium where the succession up to and including the Marra Mamba Iron Formation has been divided into 11 unconformity-bounded packages and an upper package with a basal unconformity (Blake, 2001; Fig. 2). The packages have been numbered sequentially from oldest to youngest (Figs. 2 and 3) and each is interpreted as a cogenetic unit. Importantly, packages are not hierarchically identical, and have been numbered rather than named because the full geographic extent of most of them has not yet been determined. This division represents the most sophisticated to date and divides the succession into components that are genetically more meaningful than does the available lithostratigraphy (Blake, 2001). This unconformity-based stratigraphic framework

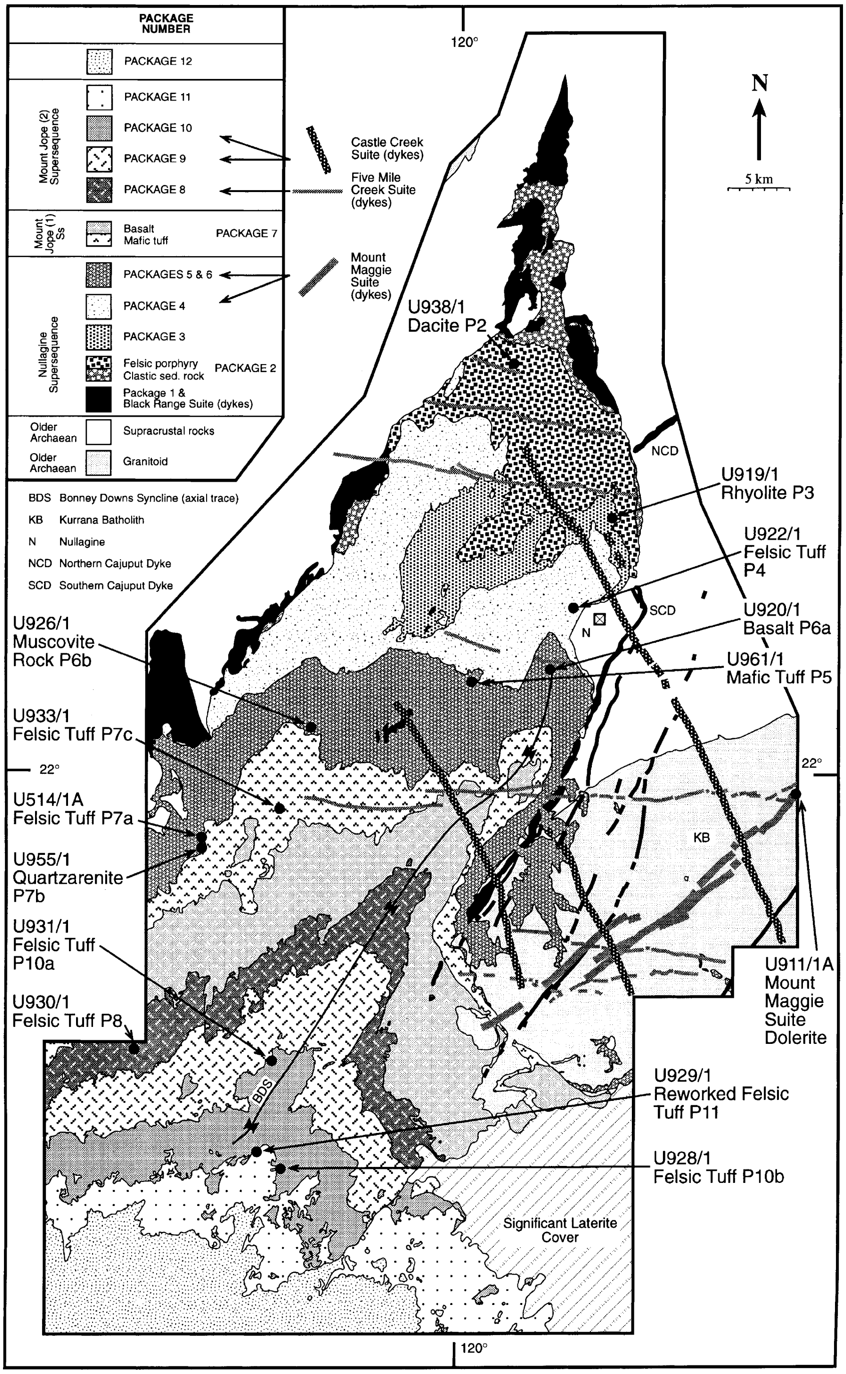

Fig. 3. Geological map of the Nullagine Synclinorium showing the distribution of packages and related dykes suites, and the locations of geochronology samples. See Blake (2001) for detailed description and chemical analyses. Arrows from dyke suites in legend show the correlations of Blake (2001).

Table 2

A summary of previous zircon U–Pb, baddeleyite U–Pb and hornblende $^{40}Ar/^{39}Ar$ geochronology of the lower succession of the Hamersley Province including intrusive and extrusive rocks

Host lithostratigraphic unit (after Thorne and Hickman, 1998)	Area (see Fig. 1)	Sample number	Age reference number	Age (Ma)	Number of grains analysed*	Interpreted meaning of age	Rock type	Mineral and method	Reference
Marra Mamba Iron Formation	Southwest Pilbara Area	120046	24	2597 ± 5	15 (15)	Age of "syndepositional volcanism"	Shale band	Zircon, SHRIMP	Trendall et al. (1998)
Jeerinah Formation	Southwest Pilbara Area (approximately)	120048	23	2629 ± 5	Not given	Not given	Andesitic ignimbrite	Zircon, SHRIMP	Trendall (unpublished data) in Nelson et al. (1999)
Jeerinah Formation	West Pilbara Basin	94776	22	2684 ± 6	11 (14)	Age of eruption	Andesitic ignimbrite	Zircon, SHRIMP	Arndt et al. (1991)
Jeerinah Formation	Southwest Pilbara Area	103225	21	2690 ± 16	13 (16)	Age of "depositionally coeval volcanism"	Tuffaceous sandstone	Zircon, SHRIMP	Arndt et al. (1991)
Tumbiana Formation	West Pilbara Basin	94775	**20**	**2715 ± 6**	28 (40)	Age of volcanism	Tuffaceous sandstone	Zircon, SHRIMP	Arndt et al. (1991)
Maddina Formation	West Pilbara Basin	144993	**19**	**2717 ± 2**	27 (27)	Age of crystallisation	Dacite	Zircon, SHRIMP	Nelson (1998)
Tumbiana Formation	West Pilbara Basin	168935	**18**	**2719 ± 6**	25 (25)	"time of igneous crystallisation for a volcanogenic component"	Volcaniclastic sandstone	Zircon, SHRIMP	Nelson (2001)
Unnamed dolerite dykes in pre-Fortescue Group granitic rocks	Sylvania Area	Z30, Z31	**17**	**2747 ± 4**	41 (46)	Emplacement of the dykes	Meta-dolerite	Zircon, SHRIMP	Wingate (1999)
Hardey Formation	Southwest Pilbara Area	2944826/6	**16**	**2750 ± 4**	32 (32)	Age of contemporaneous felsic volcanism	Siltstone with accretionary lapilli	Zircon, SHRIMP	Hall (2002)
Hardey Formation	East Pilbara Basin (Northwest Oakover Syncline)	94761	**15**	**2756 ± 8**	10 (14)	Age of "igneous activity"	Rhyolite porphyry "sill or lava"	Zircon, SHRIMP	Arndt et al. (1991)
Gregory Granitic Complex	Gregory Range Area	118924	**14**	**2757 ± 5**	18 (18)	Age of crystallisation of granite precursor	Horneblende-biotite granite augen gniess (rapakivi granite)	Zircon, SHRIMP	Nelson (1996)
Pre-Fortescue Group granitic rocks	Mount Edgar Batholith	142825	**13**	**2757 ± 7**	17 (17)	Age of crystallisation	Coarse-grained syenite	Zircon, SHRIMP	Nelson (1998)
Pre-Fortescue Group granitic rocks	Warrawagine Batholith	142875	**12**	**2758 ± 4**	18 (18)	Age of crystallisation	Quartz-feldspar porphyry dyke	Zircon, SHRIMP	Nelson (1999)
Kylena Formation	Gregory Range Area	94760	**11**	**2760 ± 10**	11 (20)	Age of "igneous activity"	Rhyolite porphyry "sill"	Zircon, SHRIMP	Arndt et al. (1991)
Gregory Granitic Complex	Gregory Range Area	118925	**10**	**2761 ± 2**	26 (26)	Age of crystallisation	Biotite monzogranite	Zircon, SHRIMP	Nelson (1999)
Gregory Granitic Complex	Gregory Range Area	118920	**9**	**2762 ± 4**	13 (13)	Age of crystallisation	Alkali granite	Zircon, SHRIMP	Nelson (1996)
Gregory Granitic Complex	Gregory Range Area	118923	**8**	**2763 ± 8**	15 (15)	Age of crystallisation	Granophyre	Zircon, SHRIMP	Nelson (1996)
Mount Roe Basalt	West Pilbara Basin	94792	**7**	**2763 ± 13**	13 (14)	Extrusive/depositional age	Grey accretionary lapilli tuff	Zircon, SHRIMP	Arndt et al. (1991)
Hardey Formation	Gregory Range Area	94759	**6**	**2764 ± 8**	12 (18)	Extrusive/depositional age	Rhyolite	Zircon, SHRIMP	Arndt et al. (1991)
Pre-Fortescue Group granitic rocks	Whim Creek Belt	118972	**5**	**2765 ± 5**	25 (25)	Age of crystallisation	Porphyritic biotite monzogranite	Zircon, SHRIMP	Nelson (1997a)
Hardey Formation	East Pilbara Basin (Nullagine Synclinorium)	77712	4	2768 ± 16	N/A	Age of crystallisation and emplacement	Quartz-dacite porphyry	Zircon, conventional	Pidgeon (1984)
Black Range dolerite suite (in pre-Fortescue Group granitic rocks)	East Pilbara Basin (Nullagine Synclinorium), Shaw Batholith, Corunna Downs Batholith, Muccan Batholith	B21, B22, B25, B28	**3**	**2772 ± 2**	68 (82)	Age of emplacement	Dolerite, gabbro	Baddeleyite, SHRIMP	Wingate (1999)
Mount Roe Basalt	Southwest Pilbara Area	86738	**2**	**2775 ± 10**	11 (11)	Extrusive/depositional age	Felsic volcanic rock	Zircon, SHRIMP	Arndt et al. (1991)
Black Range dolerite dyke (in pre-Fortescue Group granitic rocks)	Shaw Batholith	T94/29	1	2796 ± 9	N/A	Cooling age of horneblendes	Dolerite	Horneblende, $^{40}Ar/^{39}Ar$	Zegers et al. (1999)

Ages in bold in column 5 are plotted on Fig. 7. All errors are quoted as 2σ/95% confidence. Asterisk (*) indicates that the first figures show the total number of grains analysed. The figures in parentheses are the total number of areas analysed. Ages are commonly determined from selected analyses.

is used from hereon wherever possible. However, because many of the packages defined in the Nullagine Synclinorium have not yet been mapped outside this area, it is not possible to describe all LSHP rocks in terms of an unconformity-based stratigraphy of this detail. Consequently, outside the areas mapped by Blake (1990a, 2001), the lithostratigraphic nomenclature of Thorne and Hickman (1998) is used.

The Mount Bruce Megasequence Set comprises the lower Chichester Range Megasequence overlain by the Hamersley Range Megasequence (Table 1). The lower volcanic-dominated part of the Chichester Range Megasequence comprises two second-order sequences named the Nullagine Supersequence overlain by the Mount Jope Supersequence (Blake and Barley, 1992; Blake, 1993; Table 1). Blake (2001) relocated the boundaries of these two supersequences in the Nullagine Synclinorium and split the Mount Jope Supersequence in this area into the Mount Jope (1) Supersequence and Mount Jope (2) Supersequence (Figs. 2 and 3) following the palaeomagnetic study of Strik (1998). This division of the Mount Jope Supersequence has not been extended outside the Nullagine Synclinorium to date.

4. Regional geotectonic setting

The geotectonic evolution of the Nullagine and Mount Jope Supersequences has been studied by Blake (1993) and is summarised as follows. The two supersequences are interpreted as the rock record of a two-phase continental break-up in the late Archaean. The first phase, represented by the Nullagine Supersequence, was dominated by WNW–ESE directed extension that resulted in the formation of large volumes of mostly subaerial basalt (Mount Roe Sequence) followed by the development of extensional intra-continental sedimentary basins with associated felsic and mafic volcanism (Hardey Sequence Package). Uplift of the Pilbara Craton pre- and post-dated Mount Roe Sequence basaltic volcanism, and an ocean may have formed to the west of the present Craton. The second phase of break-up, represented by the Mount Jope Supersequence, involved rifting of the southern Pilbara Craton margin, possibly along the site of an earlier transfer fault, resulting in the eruption of large volumes of basalt with minor felsic volcanic rock. In the north, the craton was buried beneath subaerial flood basalt and mafic tuff piles, whereas in the south it was buried beneath a dominantly submarine mafic succession. The Nullagine/Mount Jope Supersequence boundary correlates approximately with a change from subsidence in fault-controlled basins to regional-scale subsidence and burial.

More recent studies of the Nullagine Synclinorium succession and associated mafic dykes (Strik, 1998; Blake, 2001; Strik et al., 2003) show that the second rifting episode was more complex than previously supposed and comprises the rock record of two rift phases (named Mount Jope (1) Supersequence and Mount Jope (2) Supersequence).

5. Geology of the Nullagine Synclinorium

Figs. 2 and 3 summarise the lithologies and stratigraphic divisions of the Chichester Range Megasequence in the Nullagine Synclinorium (see also Blake, 1990a, 1993, 2001). The succession comprises basalt, porphyritic felsic lava, mafic and felsic tuffs and terrigenous clastic sedimentary rock. It has been metamorphosed to very low grade (prehnite–pumpellyite–epidote zone of Smith et al., 1982), gently folded by two generations of folds and cut by a complex array of normal faults (Blake, 2001).

Packages 1–4 are dominated either by basalt (Package 1), clastic sedimentary rock and felsic porphyry (Package 2), or clastic sedimentary rock (Packages 3 and 4). Packages 5–10 are dominated by basalt and mafic tuff but also contain minor felsic tuff bands (Fig. 2). Package 11 is a marine succession that mostly consists of laminated mudrock with subordinate reworked felsic tuff, carbonated mafic volcarenite and chert. Package 12 is a marine succession that comprises laminated carbonaceous mudrock that passes gradationally upwards into ferruginous laminated chert and banded iron formation.

In addition to extrusive mafic rocks, there are four physically and geochemically distinct mafic dyke suites in the area, each with a characteristic orientation (Fig. 3). Each dyke suite can be matched geochemically to basalts within the Chichester Range Megasequence in the Nullagine Synclinorium (Blake, 2001).

6. Previous geochronology

Initial dating of the Hamersley Province succession used the Rb–Sr and Pb–Pb whole rock and mineral isochron methods which mostly yielded ages of 2300–2000 Ma (see summaries in Trendall, 1983; Blake and McNaughton, 1984; see also Nelson et al., 1992). Pidgeon (1984) published the first conventional zircon U–Pb age of 2768 ± 16 Ma for the Spinaway Porphyry (Dacite P2, see the following). Arndt et al. (1991) subsequently acquired the first ion microprobe zircon U–Pb ages from the Fortescue Group, all of which ranged between 2775 and 2684 Ma. These initial zircon U–Pb ages established a broad geochronological framework and showed that Rb–Sr and Pb–Pb isochrons obtained from igneous rocks probably date younger hydrothermal and/or metamorphic events rather than the age of magmatism (Blake and McNaughton, 1984; Nelson et al., 1992). More recently Nelson (1996, 1997a, 1998, 1999, 2001) and Hall (2002) reported a total of 10 ion microprobe zircon U–Pb ages from rocks that are probably all related to the LSHP. These ages can be split into the following three groups.

1. Three ages of ca. 2765–2757 Ma from small 'granitic' intrusions in basement rocks (Table 2, reference numbers 5, 12, 13).
2. Four ages of ca. 2763–2757 Ma from 'granitic' rocks in the Gregory Range Area (Table 2, reference numbers 8, 9, 10, 14).
3. Two stratigraphically controlled ages from the West Pilbara Basin (Table 2, reference numbers 18, 19) and one stratigraphically controlled age from the Southwest Pilbara Area (Table 2, reference number 16).

Table 2 summarises published U–Pb zircon and $^{40}Ar/^{39}Ar$ ages for the Hamersley Province succession up to and including the Marra Mamba Iron Formation.

The youngest ion microprobe zircon U–Pb age from rocks forming the basement to the LSHP is 2851 ± 2 Ma from the post-tectonic Cooglegong Adamellite in the Shaw Batholith (Nelson, 1998; Fig. 1). The Cooglegong Adamellite is intruded by the Black Range dolerite dyke (Hickman and Lipple, 1978) which is one of a suite of dykes (Black Range Suite; Fig. 1) that has been shown, using field, petrographic, geochemical and interpretive geotectonic evidence, to be cogenetic with flood basalts of Package 1 in the Nullagine Synclinorium and correlative basalts throughout the eastern Pilbara (Blake, 1993, 2001). Wingate (1999) determined a mean ion microprobe baddeleyite $^{207}Pb^{*}/^{206}Pb^{*}$ age of 2772 ± 2 Ma (Table 2, reference number 3) from four samples, each from a different dyke of the Black Range Suite including the Black Range dyke itself. This mean age for the Black Range Suite age is within the error limits of two ion microprobe zircon U–Pb ages obtained from near the base of the LSHP by Arndt et al. (1991; Table 2, reference numbers 2, 7). In contrast, Zegers et al. (1999) reports a hornblende $^{40}Ar/^{39}Ar$ age of 2796 ± 9 Ma for a sample of the Black Range dyke (Table 2, reference number 1). This is ca. 24 million years older than Wingate's Black Range dyke age (2771.6 ± 2.3 Ma) and is not within error of either of the Mount Roe Basalt ages of Arndt et al. (1991). Wingate (1999) and Zegers et al. (1999) interpret their Black Range dyke ages as "an unambiguous age of emplacement" and the "cooling age of the hornblendes in the dolerite dyke" respectively. The meaning of this discrepancy is unknown but Wingate's age is favoured here because it is more consistent with available geological evidence (Blake, 1993, 2001) and other geochronological results (Arndt et al., 1991). Existing ion microprobe geochronology therefore suggests that the time span between the last preserved major magmatic event in the basement and the oldest known basaltic magmatism in the LSHP is about 80 million years (cf. Blake, 1993).

7. The geological meaning of zircon U–Pb ages in volcaniclastic rocks

Brown and Fletcher (1999, and references therein) have documented silicic magma residence times and zircon growth of the order of hundreds of thousands of years prior to eruption. By comparison, the magma residence times of the zircons obtained in this study should be well within the errors of the most precise ages obtained (±ca. 2 million years). Therefore, concordant U–Pb ages obtained in this study from magmatic zircon populations from non-resedimented and non-reworked tuffs effectively date the age of eruption of the host rock, assuming no younger alteration.

Following eruption, pyroclastic rocks are commonly resedimented (e.g., Fisher and Smith, 1991; McPhie et al., 1993). The time between eruption and final deposition following resedimentation is usually relatively short and is probably significantly less than the most precise error limits attained by zircon ion microprobe U–Pb geochronology (±ca. 2 million years). Thus, ages from most resedimented pyroclastic rocks should generally date (within error) the time of pyroclastic volcanism. In contrast, following lithification, pyroclastic and resedimented pyroclastic deposits are commonly reworked into younger deposits. In these deposits, the time span between eruption and final deposition of the reworked deposits may be significant. Consequently, demonstrable igneous ages obtained from zircons in such rocks should be interpreted as the maximum possible age of final deposition rather than the actual age of deposition. Thus, when dating bedded fragmental volcanic deposits it is important to determine whether they are primary pyroclastic deposits, resedimented pyroclastic deposits or reworked volcanic rocks.

In this study, the units dated include examples of pyroclastic rocks, resedimented pyroclastic rocks, reworked volcanic rock and lavas. In addition, an age has been obtained from felsic-derived zircons that are interpreted as accidental grains in a younger pyroclastic mafic eruption. This contextual information was obtained from field observations, stratigraphic relationships, petrographic studies (Appendix I) and geochemical data and is an essential adjunct to understanding the meaning of the zircon ages.

8. Field sampling, SHRIMP sample preparation, analytical methods

Whole rock geochemical analyses were obtained for all but one of the sampled units prior to sampling (Fig. 4, Appendix III). All samples are from surface exposures and only fresh material was collected wherever possible. A thin section of each sample was made and examined before each sample was crushed. Any remaining weathered material was removed before crushing.

Crushed samples were milled in a tungsten-carbide ring mill such that all material passed through a 60 mesh nylon sieve, and heavy minerals were concentrated by standard heavy liquid and magnetic separation techniques. Zircon grains were hand-picked and mounted in epoxy resin with chips of the CZ3 standard zircon, and then polished down to expose the grain mid-sections. Analyses were performed using SHRIMP II at the Curtin University of Technology in Perth, Western Australia, under the general operating conditions described by Smith et al. (1998). For all samples, six data collection cycles were performed per analysis, and count times per cycle were 10 s for the ^{204}Pb, ^{206}Pb, and ^{208}Pb mass peaks and background, and 30 s for the ^{207}Pb mass peak. Analyses were referenced to multiple analyses of the CZ3 Sri Lankan zircon standard ($^{206}Pb/^{238}U = 0.0914$, corresponding to an age of 564 Ma; Pidgeon et al., 1994; Nelson, 1997a) for U/Pb calibration. Standard analyses performed throughout each session gave errors for Pb*/U that were typically less than 2.0%. Analyses that showed a high common Pb component (>2%, expressed as %f^{206} in Appendix II), more than 10% discordance, or high U contents (>350 ppm) were excluded from mean age calculations, because Nelson (1997b) reported that zircon grains with high U contents can yield spuriously young radiogenic ages suggesting Pb loss in these grains. Data corrected for common Pb (from ^{204}Pb counts) are listed in Appendix II. Errors reported for individual analyses are 1σ, while errors for mean ages are at 95% confidence.

9. Geochronology results

Geochronology results are summarised in Tables 3 and 4, and Fig. 5. Full SHRIMP isotopic and age data are presented in Appendix II. Short descriptions of the samples are given in Tables 3 and 4, with more detailed descriptions in Appendix I. The term ‘tuff’ is used herein to cover both pyroclastic rocks and resedimented pyroclastic deposits. The term ‘resedimented’ is used for extrusive fragmental volcanic deposits that have been redeposited by sedimentary processes before lithification. The term ‘reworked’ is used for volcanic deposits that have been lithified before being eroded and redeposited by sedimentary processes.

Eleven of the 14 samples yielded meaningful ages (Table 3). Sample U926/1 (Package 6 muscovite rock) yielded no zircons despite having a relatively high Zr content (Appendix I). Samples U920/1 (Package 6

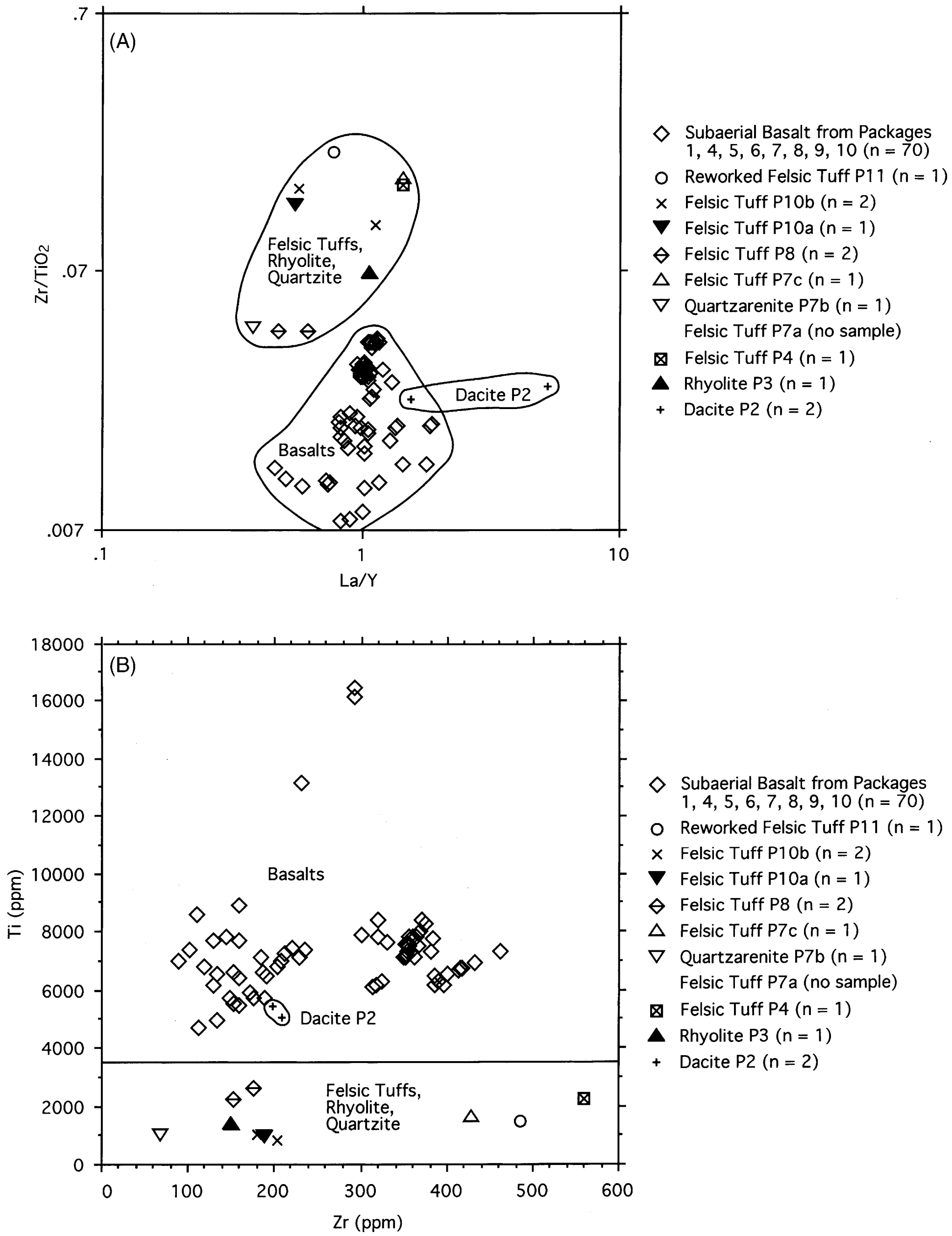

Fig. 4. Summary Zr/TiO_2–La/Y (A) and Ti–Zr (B) diagrams illustrating the geochemical differences between basalts and intermediate to felsic and reworked felsic rocks in the Nullagine and Mount Jope Supersequences in the Nullagine Synclinorium. "P" number in legend refers to package number. See Blake (2001) for basalt divisions and summary basalt analyses. Analyses of non-basaltic rocks and analytical techniques in Appendix III.

Table 3
Summary of the geochronology results in stratigraphic order, including local stratigraphic positions of samples and sample AMG coordinates

Sample number	Package number	Reference name of unit sampled	Location in package	Age (Ma) and number of analyses	Interpreted meaning of age	Mineral analysed	Sample AMG coordinate (AGD66)
U929/1	11	Reworked Felsic Tuff P11	Approximately 2.5 m above local base	2715 ± 2 (33)	Maximum age of deposition of the sandstone	Zircon	Z50 793196E 7534358N
U928/1	10	Felsic Tuff P10b	Approximately 30 m below local top, between subaerial basalt flow units	2715 ± 2 (38)	Age of eruption of volcanogenic material	Zircon	Z50 794995E 7533247N
U931/1	10	Felsic Tuff P10a	1–2 m below local top of basal mafic tuff unit	2713 ± 3 (43)	Age of eruption of volcanogenic material	Zircon	Z50 794816E 7541651N
U930/1	8	Felsic Tuff P8	Approximately 70 m above local base, between subaerial basalt flow units	2718 ± 3 (36)	Age of eruption of volcanogenic material	Zircon	Z50 783289E 7542909N
U933/1	7	Felsic Tuff P7c	Approximate centre of basal mafic tuff unit	2721 ± 4 (31)	Age of eruption of volcanogenic material	Zircon	Z50 795443E 7561178N
U955/1	7	Quartzarenite P7b	Near base of basal mafic tuff unit, possibly local basal lithology	2727 ± 5 (20)	Maximum age of deposition of the sandstone	Zircon	Z50 789231E 7558918N
U514/1A	7	Felsic Tuff P7a	Directly overlies local top basalt flow unit in Package 6	2724 ± 5 (16)	Age of eruption of volcanogenic material	Zircon	Z50 789221E 7559178N
U926/1	6	Muscovite Rock P6b	Associated with vent-like structures that post-date basalts	No zircon recovered	N/A	N/A	Z50 789016E 7568246N
U920/1	6	Basalt P6a	Local basal subaerial basalt flow unit, overlies hyaloclastite	Few zircons recovered: unsuitable for analysis (Appendix I)	N/A	N/A	Z51 197260E 7572708N
U961/1	5	Mafic Tuff P5	Approximately 5–10 m below local top of basal mafic tuff unit	2741 + 3 (26)	Maximum age of deposition of the mafic tuff	Zircon	Z51 191185E 7571407N
U911/1A	Mount Maggie Suite (dyke)	Mount Maggie Suite Dolerite	Intrudes Kurrana Batholith (correlated with top of Package 4, and Packages 5, 6; Blake, 2001)	Few baddeleyite recovered: unsuitable for analysis (Appendix I)	N/A	N/A	Z51 217293E 7563384N
U922/1	4	Felsic Tuff P4	Approximately 300 m below local top, interbedded in terrigenous clastic sedimentary rock	2752 + 5 (41)	Age of eruption of volcanogenic material	Zircon	Z51 199173E 7577333N
U919/1	3	Rhyolite P3	Base of package, approximate centre of extrusive rhyolite ?dome	2766 ± 3 (21)	Age of crystallisation	Zircon	Z51 201965E 7585039N
U938/1	2	Dacite P2	Approximately 100 m above local base of porphyry complex	2766 ± 2 (34)	Age of crystallisation	Zircon	Z51 193855E 7596766N

Table 4
Summary descriptions of sample rock types and zircon morphologies, and summary SHRIMP results for all samples except U911/1A, U920/1, U926/1

Sample number and reference name of unit sampled	Sample rock type	Zircon morphology	Summary SHRIMP results
U929/1 Reworked Felsic Tuff P11	Reworked crystal-bearing felsic tuff	Zircon grains are generally large, ranging from 60 to 450 μm, with two main morphological types. Most grains are small, colourless to light brown, euhedral to slightly rounded grains with fine magmatic zonation. Approximately 30% of grains are generally larger, light to dark brown, well-rounded grains. Most grains show evidence of some abrasion or resorption.	Thirty-seven analyses were obtained from 35 grains. Thirty-three analyses produced a single population with a mean age of 2715 ± 2 Ma (χ^2 = 0.76). Four analyses were discarded due to excessive discordance or poor precision due to low U content. The age represents the eruptive age of the volcanogenic material. Both morphological grain types were analysed.
U928/1 Felsic Tuff P10b	Fine crystal-vitric felsic tuff (most of sampled unit resedimented)	Zircon grains are generally large, ranging from 60 to 450 μm, with two main morphological types. Approximately 50% of grains are type-1: small, colourless to light brown, euhedral magmatic grains with fine growth zonation. Type-2 grains are generally larger, light to dark brown, well-rounded grains.	Forty-one analyses were obtained from 40 grains. Thirty-eight analyses produced a mean age of 2715 ± 2 Ma (χ^2 = 1.12). Three analyses gave significantly older ages (2749–2969 Ma). There is no clear relationship between age and the degree of rounding of grains. The mean age represents the eruptive age of the volcanogenic material.
U931/1 Felsic Tuff P10a	Fine crystal-vitric felsic tuff (part of sampled unit is resedimented)	Zircons are typically large (200–400 μm), euhedral prismatic grains with fine magmatic oscillatory growth zonation. Elongate mineral inclusions (?apatite) are common. Some grains (<1%) show evidence of slight abrasion. Grains are clear and colourless to pale brown in colour. No cores observed.	Forty-four analyses were obtained from 30 grains, of which one analysis was discarded due to probable Pb-loss. Forty-three analyses produced a mean age of 2713 ± 3 Ma (χ^2 = 1.11). This age represents the eruptive age of the volcanogenic material.
U930/1 Felsic Tuff P8	Fine vitric felsic hydrovolcanic tuff (part of sampled unit is resedimented)	Grains are mostly angular fragments of euhedral magmatic zircons, ranging from 50 to 250 μm in size. Whole grains are euhedral, clear and colourless to light brown, with a range in morphological types. No obvious rounding of grains or cores was observed.	Forty-two analyses were obtained from 41 grains. Six analyses were discarded due to excessive Pb-loss (discordant and/or >3σ young outliers). The remaining 36 analyses form a single population with a mean age of 2718 ± 3 Ma (χ^2 = 1.12). This age represents the eruptive age of the volcanogenic material.
U933/1 Felsic Tuff P7c	Altered fine vitric felsic tuff (part of sampled unit is resedimented)	Zircons are generally small, ranging in size from 50 to 200 μm, with two morphological types. Type-1 (90%) are euhedral, prismatic magmatic zircons that are clear and colourless to pale green, with some melt/mineral inclusions. Type-2 (10%) are generally larger (130–200 μm), and are slightly rounded and/or broken suggesting sedimentary reworking.	Thirty-one concordant analyses of type-1 zircons produced a mean age of 2721 ± 4 Ma (χ^2 = 0.97). One analysis was discarded from the mean due to excessive discordance. This age represents the eruptive age of the volcanogenic material. Two type-2 zircons gave ages of 2961 and 3301 Ma (slightly discordant).
U955/1 Quartzarenite P7b	Coarse-grained quartzofeldspathic arenite	Zircons have a size range of <100–380 μm with two main morphological types. Type-1 are clear, euhedral magmatic grains or fragments of euhedral prismatic grains with variable growth morphologies. Type-2 grains are subhedral rounded grains. The range in morphology and the presence of rounded grains suggests some sedimentary abrasion, and a variety of sources.	Thirty-one analyses were obtained from 31 grains. Twenty analyses form a single concordant population with a mean age of 2727 ± 5 Ma (χ^2 = 0.92). Five analyses were excluded from the mean due to discordance and probable Pb mobility. Six analyses form a largely discordant population at ca. 3340 Ma, indicating a significant older detrital component. There is no clear relationship between age and the degree of rounding of grains.

U514/1A Felsic Tuff P7a	Fine vitric felsic tuff (no evidence of resedimentation in sampled unit)	Zircons are generally small (<100 μm) with a small number of larger (150–180 μm) grains. There are two main morphological types. Type-1 are small, clear and colourless euhedral to slightly rounded magmatic grains. Type-2 are generally larger irregular fragments and rounded grains. The presence of rounded grains in addition to euhedral magmatic grains suggests a variety of sources, and some sedimentary abrasion.	Nineteen analyses were obtained from 19 grains. Sixteen analyses of type-1 zircons form a single concordant population with a mean age of 2724 ± 5 Ma (χ^2 = 0.80). Three analyses of type-2 grains are significantly older (3348–3407 Ma), indicating an older detrital or accidental component. The mean age of the magmatic population (type-1) represents the eruptive age of the volcanogenic material.
U961/1 Mafic Tuff P5	Mafic hydrovolcanic tuff containing an accidental felsic volcanic component (sampled unit is water-lain with minimal resedimentation)	Zircons have a size range of 50–300 μm with two main morphological types. Type-1 are euhedral prismatic magmatic grains or fragments of euhedral grains with variable growth morphologies, and common glass inclusions. Type-2 grains are subhedral and rounded grains. The range in morphology and presence of rounded grains suggests some sedimentary abrasion, and a variety of sources. Some grains appear to have cores but none were dated.	Thirty-four analyses were obtained from 34 grains. Twenty-six analyses form a concordant or near concordant population with a mean age of 2741 ± 3 Ma (χ^2 = 0.67). Seven analyses are significantly older, with ages ranging from 2813 to 3462 Ma, indicating a significant older detrital component. There is no clear relationship between age and the degree of rounding of grains.
U922/1 Felsic Tuff P4	Fine vitric felsic hydrovolcanic tuff (part of sampled unit is resedimented)	Zircons have a large range in size, from <100 to 500 μm, with most grains between 200 and 300 μm. Grains are euhedral, elongate to equant prismatic crystals, with common glass and mineral inclusions. They are generally clear and colourless to light green-brown. No obvious rounding of grains or cores was observed.	Forty-two analyses were obtained from 39 grains. Forty-one analyses produced a mean age of 2752 ± 5 Ma (χ^2 = 1.58), with the exclusion of one analysis due to probable Pb-loss. Slight excess scatter in ages is considered to reflect minor ancient Pb-loss in some grains. This age represents the eruptive age of the volcanogenic material.
U919/1 Rhyolite P3	Aphyric rhyolite	Zircons are typically 100–300 μm and are clear, pale- to dark-brown in colour. There are two main morphological types. The most abundant (type-2) are rounded, generally elongate grains, or fragments of rounded grains. Type-1 are euhedral magmatic grains. Irregular glass inclusions and embayments are common. Embayments and rounding are considered to be resorption features.	Twenty-five analyses were obtained from 25 grains. Twenty-one concordant analyses form a single population with a mean age of 2766 ± 3 Ma (χ^2 = 0.98), representing the crystallisation age of the rhyolite. Grains of both morphological types were analysed.
U938/1 Dacite P2	Porphyritic dacite	Zircons are typically 100–300 μm and are clear, pale brown, generally euhedral, elongate prismatic crystals with common glass inclusions. Some grains are slightly metamict (darker brown) and show fine magmatic growth zonation. No cores were observed.	Thirty-four analyses on 33 grains form a single population with a mean age of 2766 ± 2 Ma (χ^2 = 0.66), representing the crystallisation age of the dacite.

Arranged in stratigraphic order. See Appendix I for detailed sample descriptions and descriptions of the units sampled.

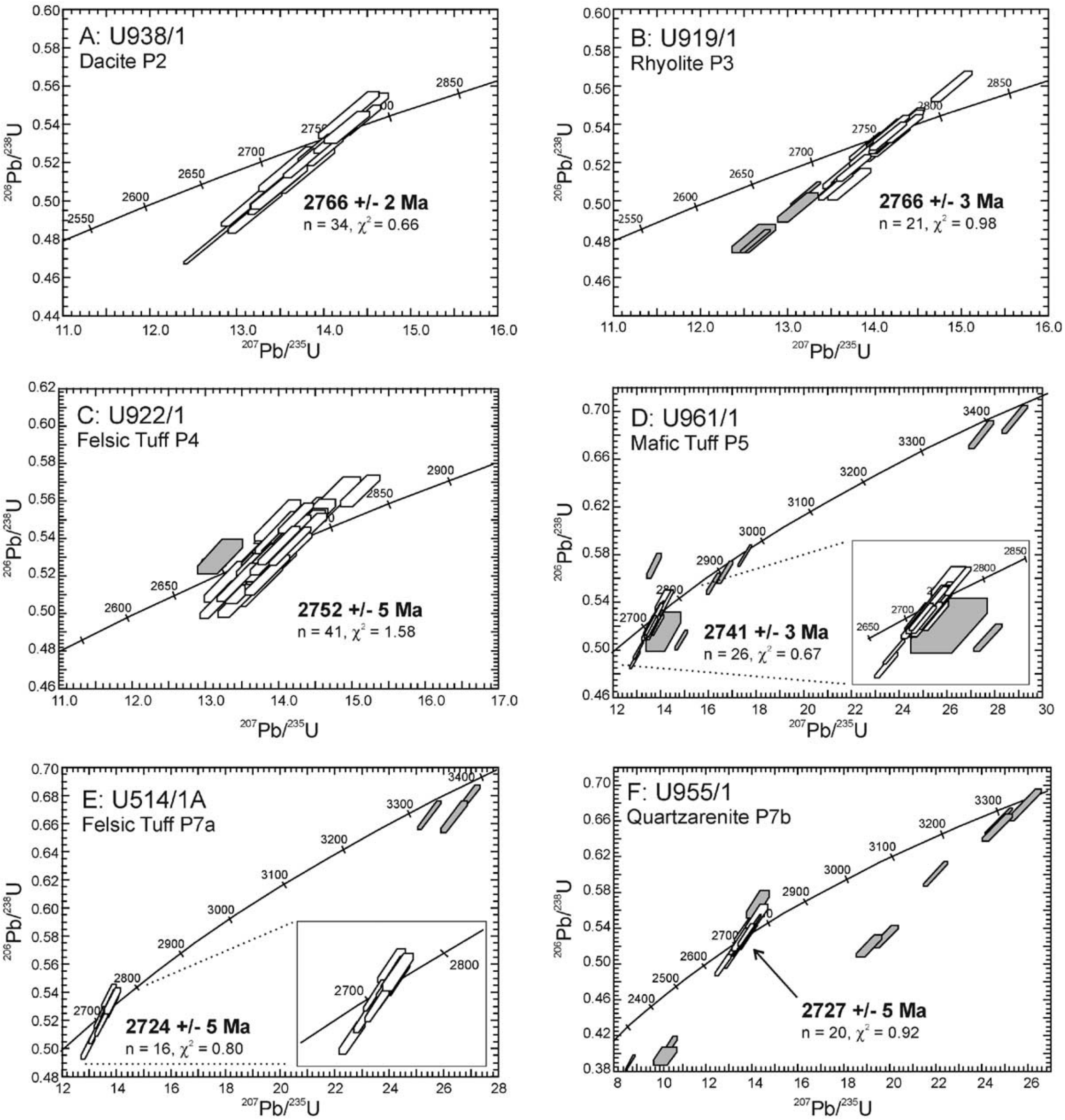

Fig. 5. Concordia plots of SHRIMP U/Pb data for all samples. Analyses plotted in grey are excluded from the mean age calculations due to excessive discordance, high U, or high common Pb contents, or they are from of an older population of zircons (see Appendix II). Some highly discordant analyses occur outside of the plotted isotopic range and are not shown. Error boxes represent 1σ. Plots are arranged in up-stratigraphic order (A–K). See Tables 3 and 4 for summary descriptions of samples, zircons and results, and Appendix II for SHRIMP data.

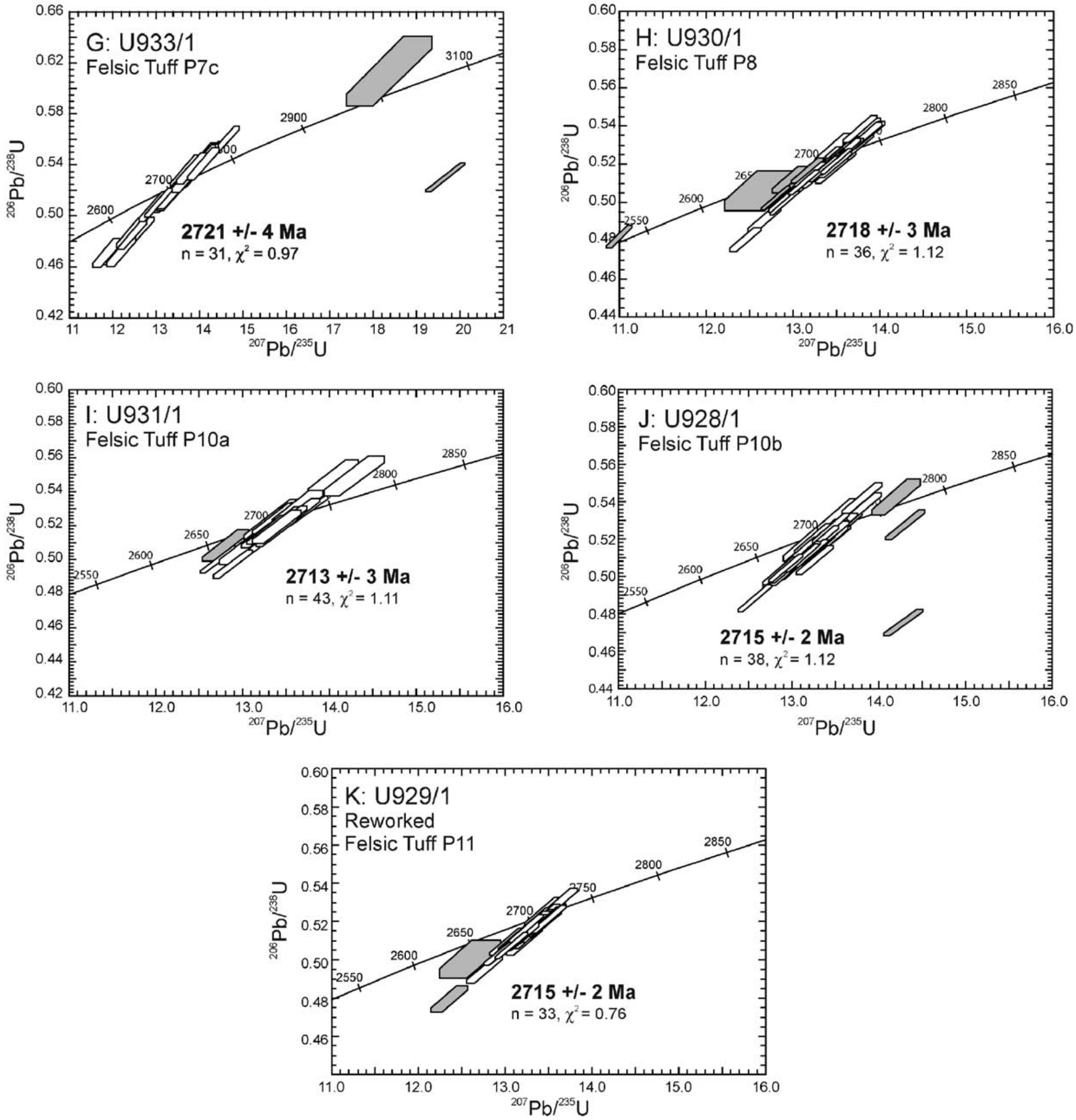

Fig. 5. (*Continued*).

basalt) and U911/1A (Mount Maggie Suite dolerite) yielded a few zircons and baddeleyites respectively, but a crystallisation age could not be determined for either sample (Appendix I). The 11 successful results are discussed briefly in the following section. Each sample has been given a descriptive name followed by its package number. Where more than one sample was taken from a package, the package number is followed by an alphabetical qualifier ordered from stratigraphic oldest to youngest.

9.1. Dacite P2 (Sample U938/1)

Dacite P2 is the Spinaway Porphyry of Lipple (1975) and is part of a porphyry complex that extends throughout the eastern Pilbara. This body is poorly understood but has an unconformable upper contact (BD3 in Fig. 2; Blake, 1990a, 1993, 2001). Sample U938/1 comes from a massive quartz-feldspar porphyry composed of about 30–40% altered feldspar, quartz and altered pyroxene. This facies is provisionally interpreted as the core of late-stage resurgent domes, possibly within a caldera (Appendix II).

The Spinaway Porphyry was dated previously at 2768 ± 16 Ma by Pidgeon (1984) using conventional zircon techniques. The mean SHRIMP age of 2766 ± 2 Ma (Tables 3 and 4; Figs. 5A and 6) confirms and refines this age, which is interpreted as the age of crystallisation of the dacite.

9.2. Rhyolite P3 (Sample U919/1)

Rhyolite P3 is up to 150 m thick and is interpreted to be a lava that erupted following initial sedimentation of Package 3 (Appendix I). The mean SHRIMP age of 2766 ± 3 Ma (Tables 3 and 4; Figs. 5B and 6) is interpreted as the age of crystallisation of the rhyolite.

9.3. Felsic Tuff P4 (Sample U922/1)

Felsic Tuff P4 is a 2.4–2.7 m thick felsic tuff horizon that is interbedded with terrigenous fluvial and alluvial fan deposits about 300 m below the top of Package 4. Most of the tuff is interpreted as the product of a hydrovolcanic eruption that was deposited as a pyroclastic surge (Appendix I). The mean SHRIMP age of 2752 ± 5 Ma (Tables 3 and 4; Figs. 5C and 6) is interpreted as the age of eruption and the effective age of deposition of the tuff.

9.4. Mafic Tuff P5 (Sample U961/1)

Mafic Tuff P5 is a 20 m thick horizon at the base of Package 5 that is chemically related to overlying basalts of the same package (Blake, 2001). The tuff is hydrovolcanic in origin and most was deposited in a lacustrine setting with minimal resedimentation. The tuff contains a significant component of accidental grains (including volcanic quartz within accretionary lapilli) that were probably entrained during explosive mafic hydrovolcanism (Appendix I). Zircons recovered from specimen U961/1 are interpreted to be part of this accidental component.

The mean SHRIMP age of 2741 ± 3 Ma of the concordant zircon population (Tables 3 and 4; Figs. 5D and 6) from Sample U961/1 is interpreted as the age of the accidental felsic volcanic component in the mafic tuff. The older zircons (2813–3462 Ma) probably represent a detrital component of clastic sediment entrained during hydrovolcanism. This interpretation implies that mafic hydrovolcanism and deposition of the mafic tuff is younger than of 2741 ± 3 Ma.

9.5. Felsic Tuff P7a (Sample U514/1A)

Felsic Tuff P7a is a thin (>3–4 cm thick) vitric tuff horizon that has been found at only one locality (U514) at the local base of Package 7. Shard morphologies suggest an explosive magmatic origin but the tuff was not welded (Appendix I). At the sample site there is no evidence that the tuff was resedimented and it appears to have filled cavities in a Package 6 subaerial flow top breccia. The mean SHRIMP age of 2724 ± 5 Ma of the concordant zircon population (Tables 3 and 4; Figs. 5E and 6) from Sample U514/1A is interpreted as the age of eruption and the effective age of deposition of the tuff. The tuff sample contains a few percent non-volcanic quartz, feldspar and schist grains that are interpreted to be accidental components rather than detrital components introduced during resedimentation (Appendix I). The older (3348–3407 Ma) zircon population probably reflects this accidental component in the tuff.

9.6. Quartzarenite P7b (Sample U955/1)

The basal few centimetres to few tens of centimetres of the basal mafic tuffs of Package 7 commonly contain detrital quartz grains throughout the Nullagine Synclinorium. Concentrations of quartz grains vary from a few scattered grains in mafic tuff to discrete ‘pockets’ of quartzarenite to quartzofeldspathic arenite. The origin of this arenite is uncertain but the interpretation favoured here (Appendix I) is that it represents the winnowed and resedimented remains of an equivalent of Felsic Tuff P7a. If so, the detrital

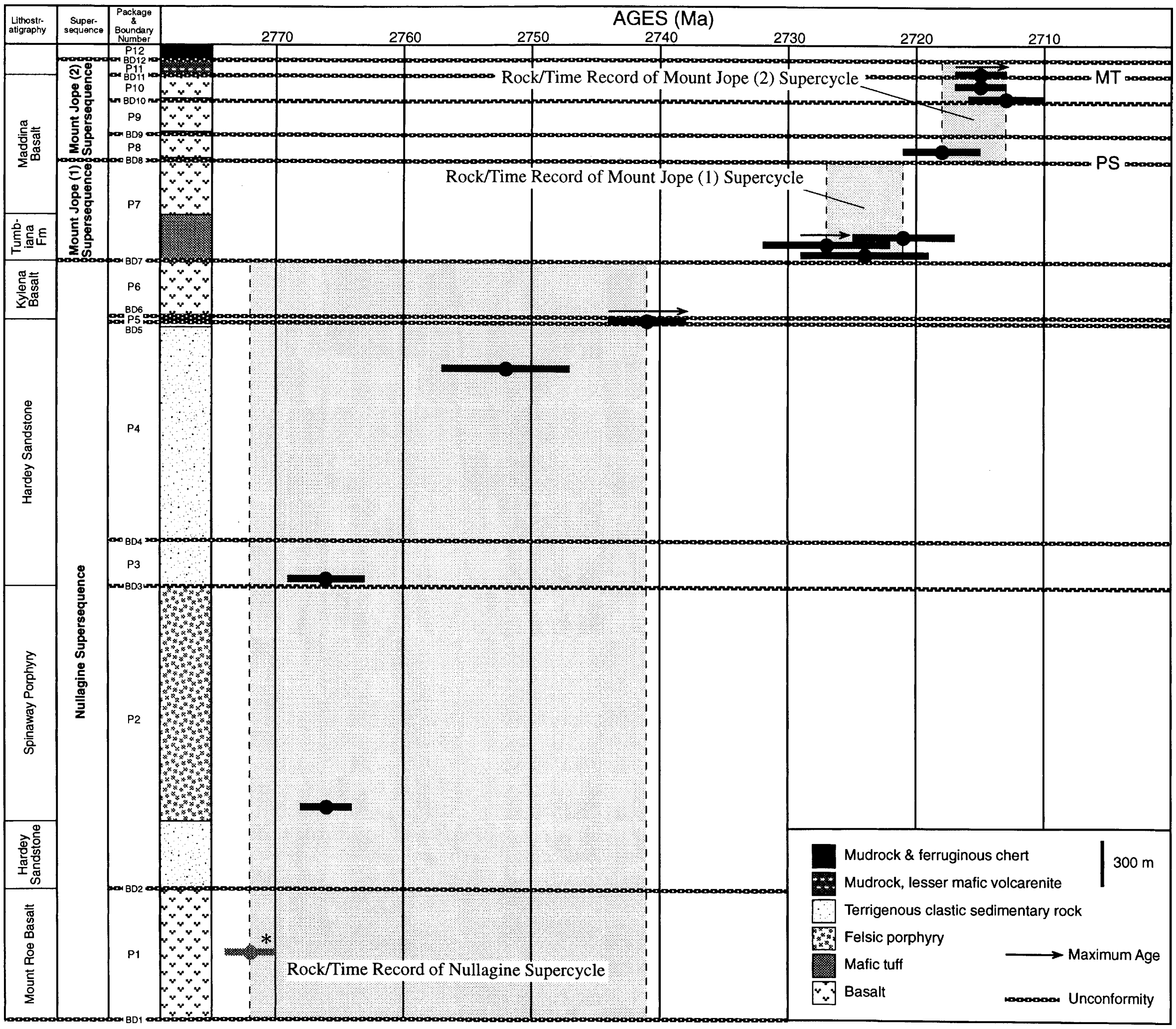

Fig. 6. A stratigraphic thickness (rock) vs. time plot for the Nullagine and Mount Jope Supersequences in the Nullagine Synclinorium. Ages are shown with 95% confidence level error bars. The grey age in P1 marked with an asterisk is the Black Range Suite dyke age of Wingate (1999; reference number 3 in Table 2) with the stratigraphic correlation of Blake (1993, 2001); all other ages are reported herein. The grey areas are a best estimate of the maximum preserved rock thickness vs. minimum time records (based on mean ages) of the Nullagine and Mount Jope Supercycles in the Nullagine Synclinorium. Right-pointing arrows indicate that the age is interpreted as a maximum age of the stratigraphic unit. All other ages are interpreted as the age of eruption of fragmental volcanic rocks or the age of crystallisation of non-fragmental felsic rocks. Lithostratigraphic nomenclature as per Fig. 2. MT, marine transgression; PS, major shift in palaeomagnetic pole position across the boundary.

quartzofeldspathic component of Quartzarenite P7b is the winnowed remains of accidental ca. 3340 Ma granitic grains from Felsic Tuff P7a and the youngest concordant zircon population of detrital zircons, dated at 2727 ± 5 Ma (Tables 3 and 4; Figs. 5F and 6), is the age of eruption of the winnowed tuff. Irrespective of the origin of Quartzarenite P7b, its age of deposition has to be younger than 2727 ± 5 Ma and older than 2721 ± 4 Ma (Felsic Tuff P7c, see the following).

9.7. *Felsic Tuff P7c (Sample U933/1)*

Felsic Tuff P7c is a discontinuous 50 cm to 1.5(?) m thick unit located near the middle of the 300 m thick mafic tuff succession at the base of Package 7 (Tumbiana Formation of Thorne and Tyler, 1996). The tuff is strongly altered but remnant volcanic textures suggest that it originated from an explosive eruption of magma containing rare quartz crystals. The presence of platy shards and accretionary lapilli indicate that the eruption involved both magmatic and hydrovolcanic processes (Appendix I). At least some of the tuff was resedimented in a shallow water setting following initial deposition. However, the preservation of intact accretionary lapilli and delicate platy shards imply minimal resedimentation.

The mean SHRIMP age of 2721 ± 4 Ma of the concordant zircon population (Tables 3 and 4; Figs. 5G and 6) from Sample U933/1 is interpreted as the age of eruption and effective age of deposition of the tuff. The two slightly discordant older (2961 Ma, 3301 Ma) zircons in the analysed population are probably accidental volcanic or xenocrystic grains rather than grains introduced during resedimentation because the tuff was deposited in a basaltic terrain.

9.8. Felsic Tuff P8 (Sample U930/1)

Felsic Tuff P8 is a distinctive accretionary lapilli-bearing felsic tuff horizon that is located between subaerial basalt flows within Package 8. The unit is mostly 1.0–1.5 m thick but may be thicker than 2.5 m in the east of the area mapped (Fig. 3). Felsic Tuff P8 is interpreted to have originated from an explosive hydrovolcanic eruption of magma containing minor quartz and possible feldspar crystals. At least some of the tuff was resedimented in a shallow water setting following initial deposition. However, the well-preserved accretionary lapilli suggest minimal aqueous transportation. The mean SHRIMP age of 2718 ± 3 Ma of the concordant zircon population (Tables 3 and 4; Figs. 5H and 6) is thus interpreted as the age of eruption and the effective age of deposition of the tuff.

9.9. Felsic Tuff P10a (Sample U931/1)

Sample U931/1 is from a felsic tuff horizon about 1–2 m below the top of an approximately 20 m thick mafic tuff unit at the base of Package 10 (Fig. 2; Blake, 2001; Kuruna Member of Thorne and Tyler, 1996). At the sample site the felsic tuff is at least 65 cm thick, but this is probably less than the original depositional thickness. The tuff contains well-preserved bubble wall shards, volcanic quartz crystals and a variety of sedimentary structures (Appendix I). Felsic Tuff P10a is interpreted to have originated from an explosive magmatic eruption of a magma that contained quartz crystals. At least some of the tuff was resedimented in a very shallow water setting following initial deposition. However, the good preservation of delicate shards and a lack of locally derived material (basaltic tuff grains) in the tuff suggest minimal resedimentation. The mean SHRIMP age of 2713 ± 3 Ma of the concordant zircon population (Tables 3 and 4; Figs. 5I and 6) from Sample U931/1 is interpreted as the age of eruption and the effective age of deposition of the tuff.

9.10. Felsic Tuff P10b (Sample U928/1)

The sampled unit is a 10–20 cm to >1.5 m thick, quartz-rich sandstone horizon that is located within the Package 10 subaerial basalt pile. At the sample site, the tuff is approximately 30 m below the top of Package 10 and is 60–75 cm thick. The tuff comprises volcanic quartz and feldspar crystals, and texturally well-preserved platy and cuspate shards. Felsic Tuff P10b is interpreted to have originated from an explosive magmatic eruption of a magma that contained quartz and feldspar crystals. Most of the tuff appears to have been resedimented in a very shallow water setting following initial deposition. However, the good preservation of delicate shards and a lack of locally derived material (basalt grains) in the tuff suggest minimal resedimentation. The mean SHRIMP age of 2715 ± 2 Ma of the concordant zircon population (Tables 3 and 4; Figs. 5J and 6) is interpreted as the age of eruption and the effective age of deposition of the tuff. Given the intra-basaltic setting, the three 2749–2969 Ma zircon grains are interpreted to be accidental or xenocrystic components of the tuff rather than grains introduced during sedimentary reworking.

9.11. Reworked Felsic Tuff P11 (Sample U929/1)

Sample U929/1 was collected from about 2.5 m above the base of a 5 m thick sandstone horizon that comprises mostly siltstone grains with some volcanic quartz grains and subrounded to rounded zircons. The unit forms the base of Package 11 and was included as part of the Woodiana Member of the Jeerinah Formation by Thorne and Tyler (1996).

The Package 10/11 unconformity (BD11 in Fig. 2) is interpreted as a marine transgression surface (Blake, 1993; Gressier, 1996) that marks the end of terrestrial deposition in the Nullagine Synclinorium but not the end of mafic volcanism (Blake, 2001). In addition to Boundary 11 marking a major change in depositional settings (from terrestrial to marine), there is field evidence that the underlying Package 10 subaerial basalt pile was eroded locally before the onset of Package 11 sedimentation (Appendix I). Reworked Felsic Tuff P11 is interpreted as a lithified felsic tuff that was reworked in a marginal to shallow marine environment. The primary tuff was apparently deposited after the eruption of Package 10 basalt, implying that it has not been reworked from Felsic Tuffs P10a or P10b (Appendix I). The mean SHRIMP age of 2715 ± 2 Ma of the concordant zircon population (Tables 3 and 4; Figs. 5K and 6) from Sample U929/1 is thus interpreted as the age of eruption of the volcanogenic component of the tuff and as the maximum age of the unit.

10. Discussion

Eleven geologically meaningful ages were obtained from the 14 samples collected from or near the Nullagine Synclinorium. Figure 6 illustrates graphically the age determinations of this study. All but three of the determinations are interpreted as ages of crystallisation or eruption (Table 4; Appendix I). The three exceptions (Mafic Tuff P5, Quartzarenite P7b, Reworked Felsic Tuff P11) are interpreted as maximum possible ages of deposition of sampled units. Figure 6 shows that, within the errors, the geochronological results accord well with stratigraphic position; i.e., they young stratigraphically upwards.

10.1. Local stratigraphic implications

The geochronology results fall into two time groups that accord with the two supersequences defined in Blake (2001). The Nullagine Supersequence is dated at between ca. 2772 Ma (Wingate, 1999) and ca. 2741 Ma, but its youngest age is not well constrained because Package 6 has not yet been dated and because the youngest age obtained from the supersequence (basal Package 5) is interpreted as a maximum age. The Mount Jope Supersequence is dated at ca. 2727–2715 Ma, but again the youngest age limit is not well-constrained because only a maximum age has been determined for the base of Package 11.

Blake (2001) showed that Packages 5 and 6 comprise subaerial basalts and lesser mafic tuffs that are chemically very similar to each other. The two packages are also genetically related and each represents a single eruptive cycle. Similar Phanerozoic successions accumulated over relatively short time periods (e.g., Hooper et al., 2002) so it is thus unlikely that the rock record of these two cycles represents more than a few million years at most. Assuming the age of the mafic tuff at the base of Package 5 is not significantly younger than the age of its igneous zircon population (2741 ± 3 Ma; see Section 9.4 and Appendix I), the age of final volcanism of the Nullagine Supersequence could be ca. 2741 Ma. This suggests that the boundary between the Nullagine and Mount Jope Supersequences in this area may be an unconformity spanning a time interval of more than 10 million years. However, until a high precision depositional age is obtained from the top of Package 6, this remains uncertain.

The difference between the mean of the youngest age within the Mount Jope (1) Supersequence (2721 Ma) and the mean of the oldest age within Mount Jope (2) Supersequence (2718 Ma) is 3 million years. However, these dates are within error allowing a range of greater than zero to ten million years for its duration.

Age determinations are still too few and too widely spaced stratigraphically to determine the time significance of all unconformities within supersequences, though Boundaries 3, 9, 10 and 11 appear relatively short (Fig. 6). This is consistent with their interpreted hierarchical positions within supersequences.

The age of the upper part of Package 4 is constrained by the maximum age of 2741 ± 3 Ma of the base of Package 5 (Fig. 2). Simple extrapolation of a mean sedimentation rate of 100 m per million years (see Section 10.3) into the upper 300 m of Package 4 suggests that the top of the Package 4 may be about 2749 Ma, leaving about an 8 million years time-gap across Boundary 5 (Fig. 2). However, geological constraints such as the interpreted cessation of basin margin faulting during deposition of the upper 300 m of Package 4 (Blake, 1993) suggest that mean sedimentation rates were probably lower than 100 m per million years in this part of the succession. In addition, the strong chemical similarities between basalts in the top of Package 4 and basalts in Packages 5 and 6 (Blake, 2001) suggest that they were all related to a single magmatic cycle. Combined, these data suggest that Boundary 5 probably represents a time break that is significantly less than the difference (11 million years) between the mean age of Felsic Tuff P4 (2752 ± 5 Ma) and the maximum age of Mafic Tuff P5 (2741 ± 3 Ma; Fig. 2).

Boundary 11 represents a marine transgression surface that marks the end of terrestrial deposition in the Nullagine Synclinorium (Blake, 1993, 2001). The reworked tuff at the base of Package 11 (Reworked Felsic Tuff P11) contains rounded zircons dated at 2715 ± 2 Ma. This age is identical to the depositional age of Felsic Tuff P10b which is interbedded with basalt only 30 m below Boundary 11. Field evidence, petrographic evidence and other geological arguments (Appendix I) indicate that Reworked Felsic Tuff P11 is not derived from Felsic Tuff P10b but rather that it is derived from a tuff of similar composition deposited after the highest preserved basalts in Package 10. This suggests that the time period represented by Boundary 11 in the Nullagine Synclinorium is within the errors of the two ages (<4 million years).

10.2. Regional stratigraphic implications

Fig. 7 is a graphic summary of all ion microprobe zircon U–Pb ages and baddeleyite $^{207}Pb^{*}/^{206}Pb^{*}$ ages from Nullagine and Mount Jope Supersequence crustal and supracrustal rocks, including the ages presented in this paper (Tables 2 and 3). For comparison, previously published ages that are stratigraphically controlled (Table 2, reference numbers 2, 6, 7, 11, 15, 18–20) have been placed within the Nullagine Synclinorium stratigraphic succession according to the correlations of Thorne and Hickman (1998), even though they were not obtained from samples from this area (see figure caption for the placing of age reference number 16). Seven out of nine of the previously published ages that are stratigraphically controlled (Table 2, reference numbers 2, 6, 7, 15, 18, 19) accord (within errors) with the new Nullagine Synclinorium rock-time framework.

An age ascribed to the Kylena Basalt in the Gregory Range Area by Arndt et al. (1991; Table 2, reference number 11, 2760 ± 10 Ma) is older than its supposed stratigraphic equivalent in the Nullagine Synclinorium (Figs. 2, 6 and 7; dated herein at < 2741 ± 3 Ma). This age was derived from a “rhyolite porphyry . . . sill (that) intrudes (the) Kylena Basalt and unnamed sediments conformably below” (Arndt et al., 1991) and therefore represents a minimum age for the intruded rocks. Thus, the Kylena Basalt in the Gregory Range Area and the Kylena Basalt in the Nullagine Synclinorium (Kylena Formation of Thorne and Hickman, 1998) are unlikely to be the same rock unit.

Arndt et al. (1991) derived a maximum depositional age of 2715 ± 6 Ma from tuffaceous sandstone in the Tumbiana Formation in the West Pilbara Basin (Table 2, reference number 20; Fig. 7). While this age is within error of a supposed stratigraphic equivalent in the Nullagine Synclinorium (basal mafic tuff of Package 7; Fig. 2), its mean age is identical to one of the ages derived from Package 10 (Fig. 7). Nelson (2001) obtained a maximum depositional age of 2719 ± 6 Ma for a tuffaceous siltstone also mapped as Tumbiana Formation about 15 km from Arndt et al.’s 2715±6 Ma sample site. According to the map of Thorne and Hickman (1998) and the description of Nelson (2001) this older (2719 Ma) sample is stratigraphically younger than 2715 Ma sample, though the 95% confidence errors overlap (Fig. 7). The meaning of these discrepancies is unclear and will only be resolved by further mapping.

The following three alternatives are currently possible.

1. The Tumbiana Formation, which is depicted by Thorne and Hickman (1998) as stretching between the Nullagine Synclinorium and the West Pilbara Basin, is a single diachronous unit.
2. The ages of the two West Pilbara Basin determinations (Arndt et al., 1991; Nelson, 2001) lie at the older end of their error ranges (Fig. 7).
3. The Tumbiana Formation of Thorne and Hickman (1998) in the Central Pilbara Area and West Pilbara Basin (Fig. 1) is an amalgam of up to four of the genetically unrelated tuff bands mapped in the Nullagine Synclinorium (basal mafic tuffs of Packages 7–10).

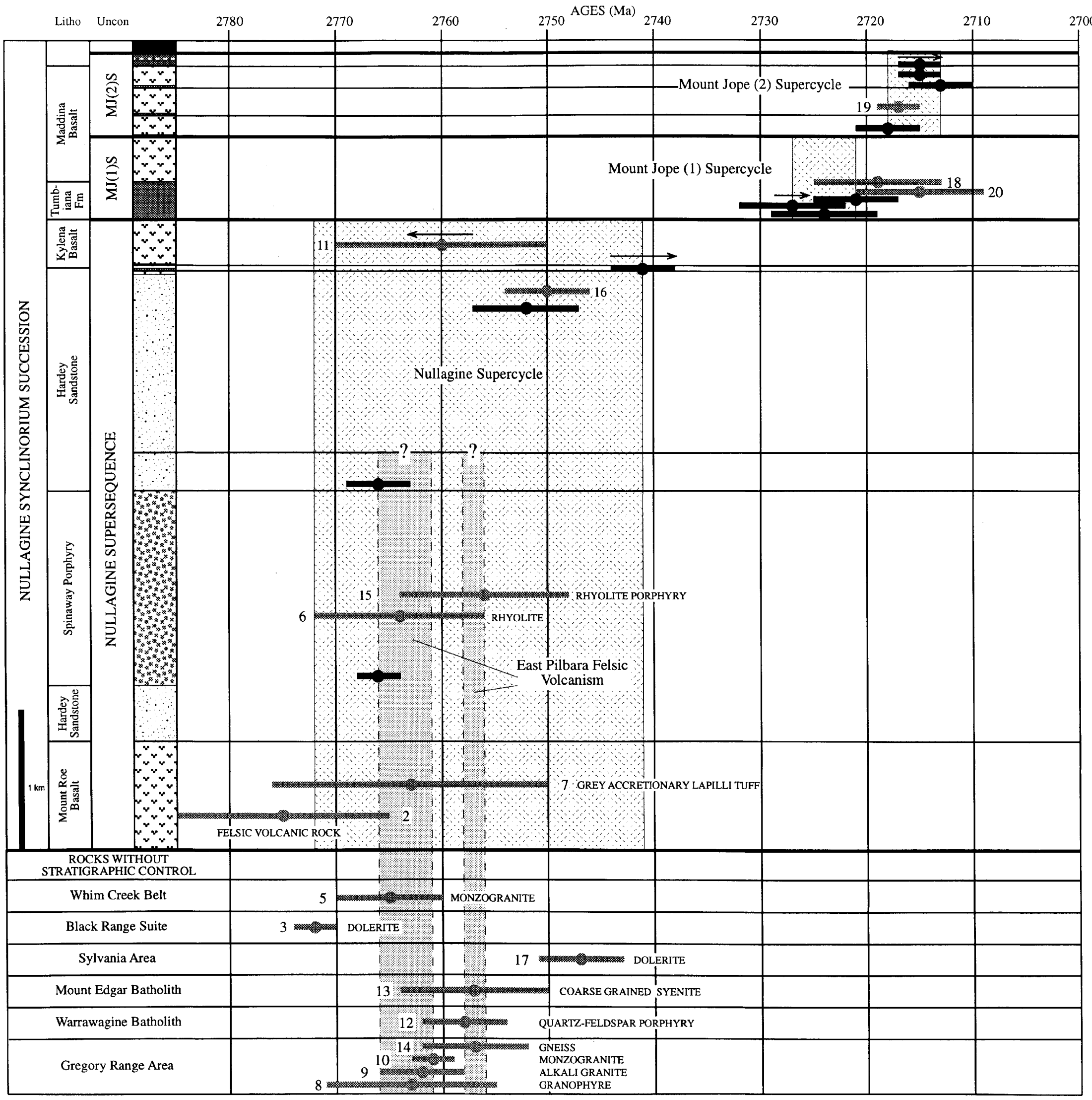

Fig. 7. Plot of published ion microprobe ages for the lower part or the Hamersley Province succession against stratigraphic position. Black dots and black 95% confidence error bars are after this study; grey dots and grey 95% confidence error bars with reference numbers are after Table 2. All ages shown in grey were obtained from samples outside the Nullagine Synclinorium. Those with stratigraphic control have been placed in the Nullagine Synclinorium succession (Figs. 2 and 6) according to the stratigraphic correlations of Thorne and Hickman (1998). The exception is number 16 (Hall, 2002) which been placed in its correct chronological position in the Nullagine Synclinorium succession rather than an equivalent local stratigraphic position (approximately 70 m above the top of the Mount Roe Basalt in the Rocklea Dome; Fig. 1). This is because placing this sample at an equivalent position in the Nullagine Synclinorium succession would be meaningless given the lateral thickness variations of the host clastic succession. Ages from samples without stratigraphic control are split by geographic areas (Fig. 1) and are ordered from east to west (bottom to top). Ages from the Gregory Range Area are ordered by decreasing mean age (bottom to top). The two grey areas are an estimate of the rock vs. minimum time record (based on mean ages) of the ca. 2766–2756 Ma east Pilbara felsic event. The left-pointing arrow on reference number 11 indicates that this is interpreted as a minimum age of the host stratigraphic unit by Arndt et al. (1991). Right-pointing arrows indicate that the age is interpreted as a maximum age of the stratigraphic unit. All other ages are interpreted as the age of eruption of fragmental volcanic rocks or the age of cooling of intrusions or lavas. Lithology legend as for Fig. 6. Column entitled “Litho” is the lithostratigraphic divisions as per Fig. 2; column entitled “Uncon” is the second-order unconformity divisions of Blake (2001). MJ(1)S, Mount Jope (1) Supersequence; MJ(2)S, Mount Jope (2) Supersequence.

Fig. 7 shows that the majority of previously published ages of felsic rocks have a mean age of between ca. 2765 and 2756 Ma. This bias in the number of age determinations reflects a volumetric abundance of suitable (for zircon U–Pb dating) felsic crustal and supracrustal rocks of this age, mostly in the eastern Pilbara. These rocks include a suite of felsic to intermediate rocks exposed throughout the East Pilbara Basin including the Spinaway Porphyry (Mapping Unit P2 of Blake, 1990a), porphyries in the Boodalyerri Creek Area (Thom et al., 1979), crustal and supracrustal 'felsic' rocks in the Gregory Range Area (Gregory Granitic Complex and Koongaling Member of Thorne and Hickman, 1998) and small granitoid plutons and dykes in the Mount Edgar Batholith, the Warrawagine Batholith and the Whim Creek area (Fig. 1; Table 2; Nelson, 1997a, 1998, 1999). Mean ages for these rocks cluster around 2766–2761 Ma and 2758–2756 Ma, though most errors overlap (Table 2; Fig. 7). This suggests that there may be two pulses of felsic magmatism (Fig. 7). Available mean ages suggest that the dated felsic rock in the Northwest Oakover Syncline of the East Pilbara Basin (2756 $\pm$ 8 Ma; Figs. 1 and 7 [reference number 15], Table 2) is younger than the base of Package 3 (Rhyolite P3, 2766 $\pm$ 3 Ma) in the Nullagine Synclinorium (also of the East Pilbara Basin). This implies that Boundary 3 in the Nullagine Synclinorium and its correlative boundary extending through the Meentheena Centrocline to the Northwest Oakover Syncline (Fig. 1; top of the Hales Grave Well Sequence of Blake, 1993, fig. 10) may be diachronous. Package 3 therefore may be unique to the Nullagine Synclinorium (Blake, 1990a, 1993, 2001). Thus, Package 3 sedimentary rocks above Rhyolite P3 (dated at 2766 $\pm$ 3 Ma) in the Nullagine Synclinorium may be a time equivalent of the younger (ca. 2756 Ma) felsic porphyry complex in the Northwest Oakover Syncline. However, this possibility needs to be tested by more detailed mapping, and high-precision geochemical and geochronological studies.

Wingate (1999) determined a mean ion microprobe zircon ^{207}Pb*/^{206}Pb* age of 2747 $\pm$ 4 Ma for two samples from two mafic dykes intruding pre-LSHP granitoids and gneisses in the Sylvania Area (Figs. 1 and 7 [reference number 17]; Table 2). This age is within error of the maximum age determined for Mafic Tuff P5 (2741 $\pm$ 3 Ma, Fig. 6). However, because the whole rock geochemistry of the Sylvania Area dykes was not presented by Wingate (1999), and because the stratigraphy and geochemistry of the LSHP in the Sylvania Area are poorly understood, no meaningful correlations, apart from broad age similarities, can yet be made between these dykes and the LSHP.

10.3. Sedimentological implications

Packages 3 and 4 comprise up to 1700 m of mostly terrigenous clastic sedimentary rocks that were deposited in braided alluvial, lacustrine and alluvial fan settings in a fault-bounded basin (Blake, 1990a, 1993). The age of 2766 $\pm$ 3 Ma of Rhyolite P3 constrains the onset of sedimentation of Package 3, and Felsic Tuff P4, dated at 2752 $\pm$ 5 Ma, is located about 300 m below the top of Package 4. These ages give a mean compacted sedimentation rate (cf. Altermann and Nelson, 1998) for this part of the succession of about 100 m per million years, though true sedimentation rates were probably greater because there is an unconformity marking the Package 3/4 boundary.

A compacted sedimentation rate of $\sim$100 m per million years rate is roughly comparable to those determined for siliciclastic fluvio-lacustrine sediments from Phanerozoic non-marine rift basins in epicontinental settings, such as the Newark Basin ($\sim$165 m per million years, Olsen and Kent, 1999). Though weathering and erosion rates should have differed substantially between Phanerozoic and late Archaean hinterlands because of marked changes in atmospheric composition and vegetation cover, this broad equivalence in compacted sedimentation rates for similar sedimentary rocks in similar settings suggests that subsidence and extension rates in fault-controlled basins were not profoundly different in the late Archaean. This implies that the underlying continental platforms were roughly comparable in thickness and rigidity.

10.4. Felsic volcanism

The work that preceded this study (e.g., Blake, 2001) showed that there are thin (few centimetres to about 1 m) felsic tuff horizons interbedded in the mafic tuffs and flood basalts of the Mount Jope Supersequence. Such tuff bands show that, on a regional scale, volcanism in this part of the succession was complex and comprised explosive mafic hydrovolcanism, subaerial and locally subaqueous flood basalt volcanism (Blake, 2001), explosive felsic magmatic volcanism and explosive felsic hydrovolcanism. The sources of the thin felsic tuff bands are unknown but they are apparently outside the Nullagine Synclinorium.

The nature of felsic tuff bands in both supersequences depends most strongly on processes that follow initial ash accumulation. Unconsolidated ashes that blanketed fluvio-lacustrine depositional systems have commonly been resedimented and/or dissected into discontinuous bodies by aqueous and possibly aeolian erosion. In contrast, felsic ashes that accumulated on the tops of flood basalt flows (Felsic Tuff P8, Felsic Tuff P10b) were preserved by burial beneath the next flood basalt flow. These tuff horizons tend to be more continuous than tuffs that accumulated in fluvio-lacustrine settings.

One of the characteristics of the zircons recovered during this study is their strongly unimodal igneous populations (Fig. 5). This is attributed in part to careful sampling following geochemical and petrographic studies. However, it is mostly due to the geological setting of the tuff bands themselves. Following emplacement of the 350 m thick Package 6 flood basalt pile there would have been little, if any, exposure of older zircon-bearing rocks such as the granite–greenstone basement or Nullagine Supersequence felsic rocks and terrigenous sandstones. Package 6 basalt contains the greatest amount of zirconium of any basalt in the Nullagine and Mount Jope Supersequences (average of 366 ppm Zr; Blake, 2001) yet only a few zircons were recovered from a Package 6 basalt Sample U920/1 (Table 3; Appendix I). It is thus unlikely that there are significant numbers of zircons in any Mount Jope Supersequence mafic rocks, apart from accidental zircons in some of the hydrovolcanic tuffs. Hence, any felsic tuff that fell into this terrain is unlikely to have incorporated an exotic zircon population during resedimentation and/or reworking.

Felsic Tuff P10a and Felsic Tuff P10b have been dated at 2713 ± 3 Ma and 2715 ± 2 Ma respectively. Petrographically (Appendix I) and geochemically (Fig. 4) these crystal-rich tuff horizons are very similar. Reworked Felsic Tuff P11 is also chemically similar to these two older tuff bands (Fig. 4A), with the few chemical differences such as relatively high Zr values possibly resulting from reworking and mechanical concentration of zircons (Fig. 4B). The eruptive age of zircons (2715 ± 2 Ma) in this reworked tuff is, within the errors, identical to the ages of Felsic Tuff P10a and Felsic Tuff P10b (Fig. 6). These geochronological, petrographic and chemical similarities, coupled with the similar thicknesses and grain size distributions of Felsic Tuff P10a and Felsic Tuff P10b suggest that all three tuffs share a similar or the same eruptive source. This may have been either a single volcano or several volcanoes of similar composition. Therefore, not only do these tuff bands prove that Package 10 basalts accumulated relatively rapidly, they also show that between 2716 and 2713 Ma, distal crystal-bearing felsic explosive magmatic volcanism accompanied the local accumulation of a mafic hydrovolcanic tuff to flood basalt pile. Such felsic tuff bands may be present outside the Nullagine Synclinorium and would make good regional time-stratigraphic markers. Moreover, they also show that there was periodic felsic volcanism accompanying mafic volcanism during all three supercycles (cf. Bryan et al., 2002; Menzies et al., 2002; Ukstins et al., 2002).

10.5. Mafic volcanism

Blake (2001) showed that the basal 20 m thick mafic tuff horizon of Package 10 and the overlying 100–150 m thick subaerial basalts of the same package form a single cogenetic unit. The top of the basal mafic tuff horizon is dated at 2713 ± 3 Ma (Felsic Tuff P10a) and ages of 2715 ± 2 Ma have been obtained from near the top of the basalt pile and immediately overlying the basalt pile (Felsic Tuff P10b, Reworked Felsic Tuff P11). These ages show that the basalt pile was deposited within a maximum period of 3 million years (2716–2713 Ma; Fig. 6). In addition, the bulk of Packages 8–10, which comprise three cogenetic mafic tuff/flood basalt couplets containing ∼500 m of basalt (Blake, 2001), was deposited over a mean interval of 3 million years (2718–2715 Ma) and a maximum period of 8 million years (between 2721 and 2713 Ma). More recent flood basalt piles of similar thickness were emplaced in less than one to a few million years (Baksi, 1989, 1994; Heimann et al., 1994; Peate, 1997; Sharma, 1997; Marzoli et al., 1999; Ernesto et al., 2002; Hooper et al., 2002; Le Gall et al., 2002). Hence, this is the first evidence for equivalent rates of emplacement of Archaean continental flood basalts.

Many oceanic and continental Phanerozoic flood basalt provinces were erupted during single, relatively short-lived (as short as <1–3 million years), geographically isolated volcanic events, and most have been attributed to mantle plumes (e.g., White and McKenzie, 1989, 1995), However, alternative mechanisms have been postulated (e.g., Anderson, 1994; King and Anderson, 1995; Sheth, 1999a,b) and some plume models have been questioned (e.g., Ernesto et al., 2002). Plume models for Phanerozoic continental flood basalt volcanism all invoke decompression melting of anomalously hot asthenospheric mantle, though in detail the relative roles of plumes, asthenosphere, continental lithospheric mantle, continental crust, lithospheric stretching and continental rifting are debated (e.g., Richards et al., 1989; White and McKenzie, 1989, 1995; White, 1992; Hooper, 1997; Lassiter and DePaolo, 1997; Peate, 1997; Saunders et al., 1997).

Though it is not known whether mantle plume activity was responsible for the late Archaean flood basalt activity, the broad similarity with eruption rates in Phanerozoic piles presumed to be of such origin might be taken to indicate a comparable generative process. However, if the Archaean upper mantle were hotter than at present, as commonly supposed (e.g., Bickle, 1978; Nisbet, 1984), anomalously hot mantle plumes would not necessarily be prerequisites for voluminous basaltic volcanism in intra-continental settings (Blake, 1993). Instead, lithospheric stretching and crustal thinning anywhere on the Archaean Earth might have generated high volumes of basaltic melt. Crustal-scale fracturing, as found in extended fault-bounded basins, could then provide plumbing adequate for emplacement. So mantle plume activity may not be the only plausible explanation for such rapid and widespread flood basalt formation in late Archaean successions (cf. Arndt et al., 2001). Further geochemical data are needed to resolve the issue.

10.6. Tectonic implications—a late Archaean drift rate?

Strik (1998) and Strik et al. (2003) have undertaken a palaeomagnetic study of rocks, mostly basalts, of the Nullagine and Mount Jope Supersequences in the Nullagine Synclinorium. Positive fold, conglomerate and reversal tests confirmed that the primary natural remanent magnetisation is preserved in these rocks, allowing a magnetostratigraphy (Fig. 2) and an apparent polar wander path (APWP) to be developed for this succession (Packages 1–10). Assuming a geocentric axial dipole and no true polar wander, the APWP shows that the Pilbara Craton was drifting between about 2772 and 2715 Ma. Most notably, Strik et al. (2003, table 1) showed a 27.2° shift in palaeolatitude between the mean palaeopoles for basalts from Packages 7 and 8, and a 26.6° shift in mean palaeolatitude between Packages 4–7 grouped and Packages 8–10 grouped (op. cit., table 3). This major shift in palaeolatitude occurs across an unconformity (BD8; Fig. 2) that also marks a significant change in basalt geochemistry (Blake, 2001, fig. 7, compare Packages 7 and 8).

Ages of 2721 ± 4 Ma and 2718 ± 3 Ma have been determined for felsic tuff bands in the basal mafic tuff of Package 7 and the lower basalts of Package 8 respectively (Fig. 2). This yields a mean time period of 3 million years and a maximum time period of 10 million years (95% confidence) between these two horizons and across the BD8 unconformity. Thus, assuming an Earth of present radius, the 27° palaeolatitudinal shift across Boundary 8 equates to a distance of about 3000 km which in 3 million years gives an apparent drift rate of about 100 cm per year. Within the 95% confidence errors of both the geochronology and the palaeomagnetic study (using data in table 3 of Strik et al., 2003), the minimum apparent drift rate is about 10 cm per year. Because the age errors overlap there is no constraint on the minimum time interval and therefore no upper limit to the apparent drift rate. Moreover, all these apparent drift rates are minimums because palaeolongitude cannot be constrained. If this is truly a measure of the rate of continental drift in the late Archaean, it ranges from extremely fast by modern standards to more than five times more rapid than the fastest rates of plate movement recorded during the last half-billion years (e.g., Meert and Tamrat, 2003).

Such a fast minimum rate of Late Archaean continental drift has profound implications for many aspects of Archaean geology. However, these inferred drift rates must be viewed with caution because there are fundamental assumptions in the interpretation of the palaeomagnetic data that cannot yet be verified independently. Alternative interpretations of the palaeomagnetic data that do not necessarily involve plate movements are possible, including contributions from non-dipole magnetic fields and true polar wander (see discussion in Strik et al., 2003).

But if the palaeomagnetic data do indeed record periodic very fast continental drift rates alternating with relative latitudinal stasis, then this implies that of the two plausible mechanisms for venting the greater Archaean heat flux, longer mid-ocean ridges or faster plate motions (Bickle, 1978), the latter was certainly involved. An alternation between very fast and relatively slow latitudinal plate motions suggests that major rearrangements of plates may have occurred more frequently in the late Archaean than at present. This pattern of movement is difficult to achieve under the current regime of very large plates and suggests that both smaller plates and faster spreading may have contributed to venting excess radiogenic heat from the late Archaean mantle.

11. Conclusions and summary

This study illustrates the benefits of combining rigorous field studies with laboratory-based research. In particular, it shows that zircon ages cannot be ascribed significant geological meaning without such a background. It is essential to understand as much as possible about the eruptive and post-eruptive histories of fragmental mafic and felsic rocks and their relationships to enclosing rocks before interpreting the meaning of the age of their zircon populations. In addition, this study and the work of Blake (2001) highlight the strengths of unconformity-based mapping and the need for unconformity-based re-mapping of most of the LSHP.

The results of this study are summarised as follows.

1. The geochronological results accord with the stratigraphic column; i.e., they young upwards (Fig. 6).
2. Unconformities represent a range of “time-gaps” that are consistent with their previously assigned hierarchical positions.
3. A mean compacted sedimentation rate of about 100 m per million years has been determined for a 1400 m thick succession of mostly terrigenous clastic sedimentary rock that was deposited in a fault-bounded extensional basin. This is similar to rates in comparable Phanerozoic settings, despite changes in constraints on sediment supply, indicating that the continental substrate to the late Archaean basin was of equivalent thickness and rigidity to younger counterparts.
4. Felsic volcanism was active intermittently for a period of about 51 million years and is an integral part of the evolution of this continental flood basalt province. While the products of proximal felsic volcanism are well-represented in parts of the succession, the products of more distal felsic volcanism are more cryptic. Nevertheless, thin distal felsic tuff bands should provide regional time markers that are essential to construction of a meaningful stratigraphic framework for the entire province.
5. At least some of the flood basalts were erupted at rates similar to those of Phanerozoic flood basalt piles, but it is still unclear whether mantle plumes were the generative force.
6. The unconformity-based stratigraphic framework, the new geochronology and palaeomagnetic studies (Strik, 1998; Strik et al., 2003) have been combined to determine a range of possible late Archaean continental drift rates for one part of the succession. If valid, such drift rates of the order of 1 m per year have far-reaching consequences for many facets of Archaean geology. However, the rates must still be viewed with caution because of fundamental uncertainties in the interpretation of the palaeomagnetic data.

Acknowledgements

We thank the following people for sample preparation, SHRIMP setup and/or analysis: Mark Doyle, Ian Fletcher, Marion Marshall, Neal McNaughton and April Pickard. This study was supported by Alkane Exploration Ltd, Ian Chalmers (Multi Metal Consultants Pty Ltd), the University of Western Australia small grant “Archaean Flood Basalt Volcanism”, ARC grant A39700939 and the NASA Astrobiology Institute. W. Altermann and S.W. Nicholson are thanked for their thorough and constructive reviews.

References

Altermann, W., Nelson, D.R., 1998. Sedimentation rates, basin analysis and regional correlations of three Neoarchaean and Palaeoproterozoic sub-basins of the Kaapvaal Craton as inferred from precise U–Pb zircon ages from volcaniclastic sediments. Sediment. Geol. 120, 225–256.

Anderson, D.L., 1994. The sublithospheric mantle as the source of continental flood basalts; the case against the continental lithosphere and plume head reservoirs. Earth Planet. Sci. Lett. 123, 269–280.

Arndt, N., Bruzak, G., Reischmann, T., 2001. The oldest continental and oceanic plateaus: Geochemistry of basalts and komatiites of the Pilbara Craton, Australia. In: Ernst, R.E., Buchan, K.L. (Eds.), Mantle Plumes: Their Identification Through Time. Geological Society of America Special Paper 352, pp. 359–387.

Arndt, N.T., Nelson, D.R., Compston, W., Trendall, A.F., Thorne, A.M., 1991. The age of the Fortescue Group, Hamersley Basin, Western Australia, from ion microprobe zircon U–Pb results. Aust. J. Earth Sci. 38, 261–281.

Ayer, J., Amelin, Y., Corfu, F., Kamo, S., Ketchum, J., Kwok, K., Trowell, N., 2002. Evolution of the southern Abitibi greenstone belt based on U–Pb geochronology: autochthonous volcanic construction followed by plutonism, regional deformation and sedimentation. Precambrian Res. 115, 63–95.

Baksi, A.K., 1989. Reevaluation of the timing and duration of extrusion of the Imnaha, Picture Gorge, and Grande Ronde Basalts, Columbia River Basalt Group. In: Reidel, S.P., Hooper, P.R. (Eds.), Volcanism and Tectonism in the Columbia River Flood-Basalt Province. Geological Society of America Special Paper 239, pp. 105–111.

Baksi, A.K., 1994. Geochronological studies on whole-rock basalts, Deccan Traps, India: evaluation of the timing of volcanism relative to the K-T boundary. Earth Planet. Sci. Lett. 121, 43–56.

Bickle, M.J., 1978. Heat loss from the Earth: a constraint on Archaean tectonics from the relation between geothermal gradients and the rate of plate production. Earth Planet. Sci. Lett. 40, 301–315.

Blake, T.S., 1984a. Evidence for stabilization of the Pilbara Block, Australia. Nature 307, 721–723.

Blake, T.S., 1984b. The lower Fortescue Group of the northern Pilbara Craton: stratigraphy and palaeogeography. In: Muhling, J.R., Groves, D.I., Blake, T.S. (Eds.), Archaean and Proterozoic Basins of the Pilbara: Evolution and Mineralization Potential. Geological Department and University of Extension, University of Western Australia, Publication 9, pp. 123–143.

Blake, T.S., 1990a. Bedrock geology of the Fortescue Group of the northern Pilbara Craton. Key Centre for Strategic Mineral Deposits. Geological Department and University of Extension, University of Western Australia Map Series 1, 10 Sheets.

Blake, T.S., 1990b. Fortescue Group stratigraphy, palaeogeography and tectonics. In: Recent Advances in Understanding the Archaean and Early Proterozoic Geology of the Pilbara Craton. Prog. and Abstr. Geological Department and University of Extension, University of Western Australia, pp. 18–24.

Blake, T.S., 1993. Late Archaean crustal extension, sedimentary basin formation, flood basalt volcanism and continental rifting: the Nullagine and Mount Jope Supersequences, Western Australia. Precambrian Res. 60, 185–241.

Blake, T.S., 2001. Cyclic continental mafic tuff and flood basalt volcanism in the late Archaean Nullagine and Mount Jope Supersequences in the eastern Pilbara, Western Australia. Precambrian Res. 107, 139–177.

Blake, T.S., Barley, M.E., 1992. Tectonic evolution of the Late Archaean to Early Proterozoic Mount Bruce Megasequence Set, Western Australia. Tectonics 11, 1415–1425.

Blake, T.S., McNaughton, N.J., 1984. A geochronological framework for the Pilbara Region. In: Muhling, J.R., Groves, D.I., Blake, T.S. (Eds.), Archaean and Proterozoic Basins of the Pilbara: Evolution and Mineralization Potential. Geological Department and University of Extension, University of Western Australia, Publication 9, pp. 1–22.

Blight, D.F., 1985. Economic potential of the lower Fortescue Group and adjacent units in the southern Hamersley Basin: a study of depositional environments. Geological Survey of Western Australia, Report 13.

Brown, S.J.A., Fletcher, I.R., 1999. SHRIMP U–Pb dating of the preeruption growth history of zircons form the 340 Ka Whakamaru Ignimbrite, New Zealand: evidence for >250 k.a. magma residence times. Geology 27, 1035–1038.

Bryan, S.E., Riley, T.R., Jerram, D.A., Stephenson, C.J., Leat, P.T., 2002. Silicic volcanism: an undervalued component of large igneous provinces and volcanic rifted margins. In: Menzies, M.A., Klemperer, S.L., Ebinbger, C.J., Baker, J. (Eds.), Volcanic Rifted Margins. Geological Society of America Special Paper 362, pp. 97–118.

Buick, R., 1992. The antiquity of oxygenic photosynthesis: evidence from stromatolites in sulphate-deficient Archaean lakes. Science 255, 74–77.

Buick, R., Brauhart, C.W., Morant, P., Thornett, J.R., Maniw, J.G., Archibald, N.J., Doepel, M.G., Fletcher, I.R., Pickard, A.L., Smith, J.B., Barley, M.E., McNaughton, N.J., Groves, D.I., 2002. Geochronology and stratigraphic relationships of the Sulphur Springs Group and Strelley Granite: a temporally distinct igneous province in the Archaean Pilbara Craton, Australia. Precambrian Res. 114, 87–120.

de la Hunty, L.E., 1965. Mount Bruce, Western Australia. Geological Survey of Western Australia, 1:250,000 Geological Series, Explanatory Notes.

Ernesto, M., Margues, L.S., Molina, E.C., Ussami, N., Comin-Chiarmonti, P., Bellini, G., 2002. Paraná Magmatic Province—Tristan da Cunha plume system: fixed versus mobile plume, petrogenetic considerations and alternative heat sources. J. Volcanol. Geotherm. Res. 118, 15–36.

Fisher, R.V., Smith, G.A., 1991 (Eds.), Sedimentation in Volcanic Settings. SEPM Special Publication 45, 257 pp.

Goddard, A.B., 1992. The Depositional Style and Tectonic Setting of the Early Proterozoic Turee Creek Group in the Hardey Syncline, Hamersley Province, Northwestern Western Australia. B.Sc. Honours Thesis. University of Western Australia, Perth.

Gressier, J.M., 1996. The Transition Between the Fortescue and Hamersley Groups in the Nullagine Synclinorium, Western Australia: Implications for Late Archaean Evolution of the Pilbara Craton. B.Sc. Honours Thesis. University of Sydney, Sydney, Australia.

Hall, C.E., 2002. Sedimentology, Geochemistry and Palaeogeography of the Lower Fortescue Group, Hamersley Province, Western Australia. Ph.D. Thesis. University of Western Australia, Perth, Australia.

Heimann, A., Fleming, T.H., Elliot, D.H., Foland, K.A., 1994. A short interval of Jurassic continental flood basalt volcanism in Antarctica. as demonstrated by $^{40}Ar/^{39}Ar$ geochronology. Earth Planet. Sci. Lett. 121, 19–41.

Hickman, A.H., 1978. Nullagine, Western Australia. Geological Survey of Western Australia, 1:250,000 Geological Series, Explanatory Notes.

Hickman, A.H., Lipple, S.L., 1978. Marble Bar, Western Australia. Geological Survey of Western Australia, 1:250,000 Geological Series, Sheet SF50-8.

Hooper, P.R., 1997. The Columbia River Flood Basalt Province: current status. In: Mahoney, J.J., Coffin, M.F. (Eds.), Large Igneous Provinces, Continental, Oceanic and Planetary Flood Volcanism. American Geophysical Union, Geophysical Monograph 100, pp. 1–27.

Hooper, P.R., Binger, G.B., Lees, K.R., 2002. Ages of the Steens and Columbia River flood basalts and their relationship to extension-related calc-alkaline volcanism in eastern Oregon. Geol. Soc. Am. Bull. 114, 43–50.

King, S.D., Anderson, D.L., 1995. An alternative mechanism of flood basalt formation. Earth Planet. Sci. Lett. 136, 269–279.

Krapez, B., 1996. Sequence-stratigraphic concepts applied to the identification of basin-filling rhythms in Precambrian successions. Aust. J. Earth Sci. 43, 355–380.

Krapez, B., 1997. Sequence-stratigraphic concepts applied to the identification of depositional basins and global tectonic cycles. Aust. J. Earth Sci. 44, 1–36.

Kriewaldt, M., 1964. The Fortescue Group of the Roebourne region, north-west division. Geological Survey of Western Australia, Annual Report 1963, 30–34.

Kriewaldt, M., Ryan, G.R., 1967. Pyramid, Western Australia. Geological Survey of Western Australia, 1:250,000 Geological Series, Explanatory Notes.

Lassiter, J.C., DePaolo, D.J., 1997. Plume/lithosphere interaction in the generation of continental and oceanic flood basalts: chemical and isotopic constraints. In: Mahoney, J.J., Coffin, M.F. (Eds.), Large Igneous Provinces, Continental, Oceanic and Planetary Flood Volcanism. American Geophysical Union, Geophysical Monograph 100, pp. 335–355.

Le Gall, B., Tshoso, G., Jourdan, F., Féraud, G., Bertrand, C., Tiercelin, J.J., Kampunzu, A.B., Modisi, M.P., Dyment, J., Maia, M., 2002. $^{40}Ar/^{39}Ar$ geochronology and structural data from the giant Okavango and related mafic dyke swarms, Karoo igneous province, northern Botswana. Earth Planet Sci. Lett. 202, 595–606.

Lipple, S.L., 1975. Definitions of new and revised stratigraphic units of the eastern Pilbara Region. Geological Survey of Western Australia, Annual Report 1974, 59–63.

MacLeod, W.N., de la Hunty, L.E., 1965. Roy Hill, Western Australia. Geological Survey of Western Australia, 1:250,000 Geological Series, Sheet SF 50-12.

MacLeod, W.N., de la Hunty, L.E., 1966. Roy Hill, Western Australia. Geological Survey of Western Australia, 1:250,000 Geological Series, Explanatory Notes.

MacLeod, W.N., de la Hunty, L.E., Jones, W.R., Halligan, R., 1963. A preliminary report on the Hamersley Iron Province, North-west Division. Geological Survey of Western Australia, Annual Report 1962, 44–54.

Mann, J.D., 1995. The Kylena Sequence in the Nullagine Synclinorium, East Pilbara Basin, Western Australia. B.Sc. Honours Thesis. University of Western Australia, Perth.

Marzoli, A., Renne, P.R., Piccirillo, E.M., Ernesto, M., De Min, A., 1999. Extensive 200-million-year-old continental flood basalts of the Central Atlantic Magmatic Province. Science 284, 616–618.

McPhie, J., Doyle, M., Allen, R., 1993. Volcanic Textures: A Guide to the Interpretation of Textures in Volcanic Rocks. Centre for Ore Deposit and Exploration Studies, University of Tasmania.

Meert, J.G., Tamrat, E., 2003. A mechanism for explaining rapid continental motion in the late Neoproterozoic. In: Eriksson, P.G., et al. (Eds.), The Precambrian Earth: Tempos and Events. Elsevier Publications, Amsterdam.

Menzies, M.A., Klemperer, S.L., Ebinbger, C.J., Baker, J., 2002. Characteristics of rifted margins. In: Menzies, M.A., Klemperer, S.L., Ebinbger, C.J., Baker, J. (Eds.), Volcanic Rifted Margins. Geological Society of America Special Paper 362, pp. 1–14.

Mueller, W.U., Mortensen, J.K., 2002. Age constraints and characteristics of subaqueous volcanic construction, the Hunter Mine Group, Abitibi greenstone belt. Precambrian Res. 115, 119–152.

Nelson, D.R., 1996. Compilation of SHRIMP U–Pb zircon geochronology data, 1995. Geological Survey of Western Australia, Record 1996/5.

Nelson, D.R., 1997a. Compilation of SHRIMP U–Pb geochronology data, 1996. Geological Survey of Western Australia, Record 1997/2.

Nelson, D.R., 1997b. Evolution of the Archaean granite–greenstonel terranes of the Eastern Goldfields, Western Australia: SHRIMP U–Pb zircon constraints. Precambrian Res. 83, 57–81.

Nelson, D.R., 1998. Compilation of SHRIMP U-Pb zircon geochronology data, 1997. Geological Survey of Western Australia, Record 1998/2.

Nelson, D.R., 1999. Compilation of geochronology data, 1998. Geological Survey of Western Australia, Record 1999/2.

Nelson, D.R., 2001. Compilation of geochronology data, 2000. Geological Survey of Western Australia, Record 2001/2.

Nelson, D.R., Trendall, A.F., de Laeter, J.R., Grobler, N.J., Fletcher, I.R., 1992. A comparative study of the geochemical and isotopic systematics of late Archaean flood basalts from the Pilbara and Kaapvaal Cratons. Precambrian Res. 54, 231–256.

Nelson, D.R., Trendall, A.F., Altermann, W., 1999. Chronological correlations between the Pilbara and Kaapvaal cratons. Precambrian Res. 97, 165–189.

Nisbet, E.G., 1984. Modelling mantle temperatures during the Archaean. Nature 309, 110.

Olsen, P.E., Kent, D.V., 1999. Long-period Milankovitch cycles from the Late Triassic and Early Jurassic of eastern North America and their implications for the calibration of the early Mesozoic time-scale and the long-term behavior of the planets. Phil. Trans. R. Soc. Lond. A 357, 1761–1786.

Peate, D.W., 1997. The Paraná-Etendeka Province. In: Mahoney, J.J., Coffin, M.F. (Eds.), Large Igneous Provinces, Continental, Oceanic and Planetary Flood Volcanism. American Geophysical Union, Geophysical Monograph 100, pp. 217–245.

Pidgeon, R.T., 1984. Geochronological constraints on early volcanic evolution of the Pilbara Block, Western Australia. Aust. J. Earth Sci. 31, 237–242.

Pidgeon, R.T., Furfaro, D., Kennedy, A.K., Nemchin, A.A., Van Bronswjk, W., 1994. Calibration of zircon standards for the Curtin SHRIMP II. Abstracts of the 8th International Conference on Geochronology, Cosmochronology, and Isotope Geology, Berkeley, USA. U.S. Geological Survey Circular 1107, p. 251.

Rasmussen, B., Buick, R., 1999. Redox state of the Archean atmosphere: evidence from detrital heavy minerals in ca. 3250–2750 Ma sandstones from the Pilbara Craton, Australia. Geology 27, 115–118.

Richards, M.A., Duncan, R.A., Courtillot, V.E., 1989. Flood basalts and hot spot tracks: plume heads and tails. Science 246, 103–107.

Saunders, A.D., Fitton, J.G., Kerr, A.C., Norry, M.J., Kent, R.W., 1997. The North Atlantic Igneous Province. In: Mahoney, J.J., Coffin, M.F. (Eds.), Large Igneous Provinces, Continental, Oceanic and Planetary Flood Volcanism. American Geophysical Union, Geophysical Monograph 100, pp. 45–93.

Scott, C.R., Mueller, W.U., Pilote, P., 2002. Physical volcanology, stratigraphy, and lithogeochemistry of an Archean volcanic arc: evolution from plume-related volcanism to arc rifting of SE Abitibi Greenstone Belt, Val d'Or, Canada. Precambrian Res. 115, 223–260.

Sharma, M., 1997. Siberian Traps. In: Mahoney, J.J., Coffin, M.F. (Eds.), Large Igneous Provinces, Continental, Oceanic and Planetary Flood Volcanism. American Geophysical Union, Geophysical Monograph 100, pp. 273–295.

Sheth, H.C., 1999a. Flood basalts and large igneous provinces from deep mantle plumes: fact. Tectonophysics 311, 1–29.

Sheth, H.C., 1999b. A historical approach to continental flood basalt volcanism: insights into pre-volcanic rifting, sedimentation, and early alkaline magmatism. Earth Planet. Sci. Lett. 168, 19–26.

Simonson, B.M., Schubel, K.A., Hassler, S.W., 1993. Carbonate sedimentology of the early Precambrian Hamersley Group of Western Australia. Precambrian Res. 60, 287–335.

Skulski, T., Percival, J.A., 1996. Allochthonous 2.78 Ga oceanic plateau slivers in a 2.72 Ga continental arc sequence: Vizien greenstone belt, northeastern Superior Province, Canada. Lithos 37, 163–179.

Smith, R.E., Perdrix, J.L., Parks, T.C., 1982. Burial metamorphism in the Hamersley Basin, Western Australia. J. Petrol. 23, 75–102.

Smith, J.B., Barley, M.E., Groves, D.I., Krapez, B., McNaughton, N.J., Bickle, M.J., Chapman, H.J., 1998. The Sholl Shear Zone, West Pilbara: evidence for a domain boundary structure from integrated tectonostratigraphic analyses, SHRIMP U–Pb dating and isotopic and geochemical data of granitoids. Precambrian Res. 88, 143–171.

Strik, G., 1998. Palaeomagnetism on Late Archaean Flood Basalts and Dykes of the Fortescue Group, Pilbara, Western Australia. M.Sc. Thesis. University of Utrecht, Utrecht.

Strik, G., Blake, T.S., Zegers, T.E., White, S.E., Langereis, C.G., 2003. Palaeomagnetism of flood basalts in the Pilbara Craton, Western Australia: Late Archaean continental drift and the oldest known reversal of the geomagnetic field. J. Geophys. Res. 108, B12, 2551, EMP 2-1–2-21.

Thom, R., Hickman, A.H., Chin, R.J., 1979. Nullagine, Western Australia. Geological Survey of Western Australia, 1:250,000 Geological Series, Sheet SF 51-5.

Thorne, A.M., Hickman, A.H., 1998. Geology of the Fortescue Group, Pilbara Craton. Geological Survey of Western Australia, Bulletin 144, Plates 1A–C.

Thorne, A.M., Trendall, A.F., 2001. Geology of the Fortescue Group, Pilbara Craton, Western Australia. Geological Survey of Western Australia, Bulletin 144, 249 pp.

Thorne, A.M., Tyler, I.M., 1996. Roy Hill, Western Australia. Geological Survey of Western Australia, 1:250,000 Geological Series, Sheet SF 50-12.

Tomlinson, K.Y., Davis, D.W., Percival, J.A., Hughes, D.J., Thurston, P.C., 2002. Mafic to felsic magmatism and crustal recycling in the Obonga Lake greenstone belt, western Superior Province: evidence from geochemistry, Nd isotopes and U–Pb geochronology. Precambrian Res. 114, 295–325.

Trendall, A.F., 1975. Preliminary geochronological results from two Pilbara porphyry bodies. Geological Survey of Western Australia, Annual Report, 1974, pp. 103–106.

Trendall, A.F., 1979. A revision of the Mount Bruce Supergroup. Geological Survey of Western Australia, Annual Report, 1978, pp. 63–71.

Trendall, A.F., 1983. The Hamersley Basin. In: Trendall, A.F., Morris, R.C. (Eds.), Iron-formation: Facts and Problems. Elsevier, Amsterdam, pp. 69–129.

Trendall, A.F., 1990. Hamersley Basin. In: Geology and Mineral Resources of Western Australia. Geological Survey of Western Australia, Memoir 3, pp. 163–190.

Trendall, A.F., 1997. A model for the depositional chronology of the Hamersley Basin based on zircon U–Pb ages. In: Advances in Understanding the Hamersley Province. Department of Geology and Geophysics (Key Centre), University of Western Australia, Perth.

Trendall, A.F., Nelson, D.R., de Laeter, J.R., Hassler, S.W., 1998. Precise zircon U–Pb ages from the Marra Mamba Iron Formation and the Wittenoom Formation, Hamersley Group, Western Australia. Aust. J. Earth Sci. 45, 137–142.

Ukstins, I.A., Renne, P.R., Wolfenden, E., Baker, J., Ayalew, D., Menzies, M., 2002. Matching conjugate volcanic rifted margins: $^{40}Ar/^{39}Ar$ chrono-stratigraphy of pre- and syn-rift bimodal flood volcanism in Ethiopia and Yemen. Earth Planet. Sci. Lett. 198, 289–306.

White, R.S., 1992. Magmatism during and after continental break-up. In: Storey, B.C., Alabaster, T., Pankhurst, R.J. (Eds.), Magmatism and the Causes of Continental Break-up. Geological Society Special Publication 68, pp. 1–16.

White, R., McKenzie, D., 1989. Magmatism at rift zones: the generation of volcanic continental margins and flood basalts. J. Geophys. Res. 94, 7685–7727.

White, R.S., McKenzie, D., 1995. Mantle plumes and flood basalts. J. Geophys. Res. 100, 17543–17585.

Williams, I.R., 1968. Yarraloola, Western Australia. Geological Survey of Western Australia, 1:250,000 Geological Series, Explanatory Notes.

Williams, I.R., Chin, R.J., 1987. Balfour Downs, Western Australia. Geological Survey of Western Australia, 1:250,000 Geological Series, Sheet SF 51-9.

Wingate, M.T.D., 1999. Ion microprobe baddeleyite and zircon ages for late Archaean mafic dykes of the Pilbara Craton, Western Australia. Aust. J. Earth Sci. 46, 493–500.

Wyman, D., Hollings, P., 1998. Long-lived mantle-plume influence on an Archean protocontinent: geochemical evidence from the 3 Ga Lumby Lake greenstone belt, Ontario, Canada. Geology 26, 719–722.

Zegers, T.E., Wijbrans, J.R., White, S.H., 1999. $^{40}Ar/^{39}Ar$ age constraints on tectonothermal events in the Shaw area of the eastern Pilbara granite–greenstonel terrain (W Australia): 700 Ma of Archean tectonic evolution. Tectonophysics 311, 45–81.